LARGE-SCALE ELECTRIC FIELDS AND CURRENTS AND RELATED GEOMAGNETIC VARIATIONS IN THE QUIET PLASMASPHERE

C.-U. WAGNER, D. MÖHLMANN, and K. SCHÄFER

Zentralinstitut für solar-terrestrische Physik der AdW der DDR DDR-1199 Berlin, Rudower Chaussee 5, D.D.R.

V. M. MISHIN and M. I. MATVEEV

Institute for Terrestrial Magnetism, Ionosphere and Radiowave Propagation, Sibirian Dept. of the Academy of Sciences of the USSR, Irkutsk, U.S.S.R.

(Received 10 March, 1980)

Abstract. At the end of the sixties it became obvious that two-dimensional dynamo models can explain nearly all facts, which had been found morphologically for mean annual *Sq*-fields. During the recent decade new or improved methods to measure electric fields (e.g. incoherent scatter facilities) and to investigate great data files have been developed. New informations received with these methods about the existence of regular variations of the *Sq*-field in dependence on season and universal time and about the electric field have been summarized in Section 2. All attempts to describe also these variations with a two-dimensional dynamo model did not lead to any success, but showed a strong theoretical overestimation of the asymmetries. Therefore, it must be concluded that three-dimensional plasmaspheric current systems, taking into consideration the coupling between both hemispheres along the high-conducting magnetic field lines, are needed in order to explain the regular variations of the *Sq*-field. The basic equations for two- and three-dimensional dynamo models, different methods for the solution of these equations and the resulting models from different authors are compiled and discussed (Section 3).

Based on all morphological and theoretical results a plasmaspheric-ionospheric current system has been constructed and some properties of the plasmaspheric field-aligned current distribution have been derived.

Contents

1. Introduction
   1.1. Generating processes for the electric fields
2. Regular variations of electric field and currents and related magnetic variations
   2.1. Contribution of different sources to the *Sq*-variations and plasmaspheric electric fields
   2.2. Longitudinal (UT) and seasonal variations of *Sq*-current systems
      2.2.1. Longitudinal or UT-variations of the *Sq*-field
      2.2.2. UT-variations of the electric conductivity-tensor
      2.2.3. Seasonal variations of the *Sq*-field
      2.2.4. Seasonal variation of the conductivity
      2.2.5. Summary of the most important facts and construction of an empirical three-dimensional model for the *Sq*-currents
3. Large-scale dynamo-electric fields and currents
   3.1. Symmetric dynamo-electric fields
      3.1.1. An analytical solution
      3.1.2. A simplified potential equation
      3.1.3. Numerical solution for the electrostatic potential
      3.1.4. Results of the two-dimensional symmetric dynamo models

Space Science Reviews **26** (1980) 391–446. 0038-6308/80/0264-0391 $08.40.

3.2. Three-dimensional plasmaspheric current systems
3.2.1. Basic equations
3.2.2. Reuslts
4. Summary

1. Introduction

The aim of this review paper is to summarize our knowledge about large-scale electric fields and currents and the magnetic variations resulting from these currents in the mid-latitudinal ionosphere and the plasmasphere during undisturbed conditions, i.e. to review the electrodynamics or electrostatics of large-scale phenomena within these parts of the magnetosphere and ionosphere. There are three reasons to summarize the present knowledge in this special field of research:

– During recent years a great number of new interesting morphological and theoretical results have been received by different groups. Many of these papers have been published in journals of more or less regional distribution or in russian language. A critical review of these results leads to some new very interesting conclusions.

– Incoherent backscatter measurements in mid-latitudes gave already new and more detailed informations about the electric field in this region. These measurements open new aspects for the electrostatics of the ionospheric and magnetospheric plasma. More coordinated observations of all existing stations started during the last two years, promising more detailed results (for instance about seasonal variations). Therefore it seems to be useful to summarize our present knowledge about seasonal and UT-variations of electric fields and currents.

– It has already been possible to measure field-aligned currents in higher latitudes. A further improvement of the sensitivity of these measurements would give the possibility to detect also field-aligned currents of smaller intensity in other regions. It would be interesting to know what kind of field-aligned currents one should expect from indirect indications.

For more than a century ground-based magnetic measurements taken at many observatories in different latitudes presented the only information concerning electrodynamics in ionosphere and magnetosphere. A very great amount of information is concentrated within these measurements. In order to derive from ground-based magnetic observations informations suitable for the discussion of the electrostatics or electrodynamics in the plasmasphere it must be taken into consideration that these geomagnetic variations are an integral parameter, i.e., that the geomagnetic variations measured on ground are a superposition of some outer and inner magnetic fields. Therefore, the different contributions must be separated. Since in this review, we are only interested in quiet conditions in the plasmasphere, we have to investigate S_q and S_q^p types of geomagnetic variations. It is wellknown, how to separate the inner and the outer part of the geomagnetic field (see Chapman and Bartels, 1940). Concerning the outer part of the magnetic field variations one has to

investigate, whether the magnetic fields are build up only within the plasmasphere or whether there are additional contributions from currents flowing in the outer magnetosphere, e.g. near the magnetopause. This question will be discussed in Section 2.

During recent years also measurements of the electric field within the mid-latitudinal ionosphere by direct measurements and within the plasmasphere by indirect measurements became available. These measurements gave the possibility to extract a first raw approximation for a median model of the dependence on local time and latitude (see Section 2). There are effects indicating the existence of seasonal variations of the electrostatic potential in the ionosphere. For quiet conditions the measurements seem to show that a penetration of the electric field from high latitudes into mid-latitudinal regions is very unprobable, but for the night-time conditions such a penetration is open for further discussion. From the plasmasphere the dependence of the potential in the equatorial plane in dependence on local time is known in a first approximation including some details, as for instance, the noon-bulge and the afternoon-bulge. For the day-time all results speak for a coupling between the ionosphere and the plasmasphere, but for the night-time some decouplings cannot be excluded. For more details see other reviews as Blanc and Amayenc (1976), Wagner and Schäfer (1980).

1.1. Generating processes for the electric fields

Concerning the generator for these electric fields it became clear that in principle, there are at least two different types of processes. One generator called 'the atmospheric dynamo' is situated in those ionospheric regions, where the different collisions between neutral particles and electrons on one side, and neutral particles and ions on the other lead to a different motion of ions and electrons across the magnetic field and consequently to a charge separation.

For high latitudes the measurements have shown that this generator process cannot be the main source for the electric fields. The main contributions for these latitudes come from a second type of generators – the magnetospheric dynamo processes – located far away from the Earth in the neighbourhood of the magnetopause and the magnetospheric tail. A detailed discussion of these processes is out of the scope of this paper.

In the following the physical mechanism of the atmospheric dynamo will be discussed more in detail, but without a quantitative treatment, which is reserved for section 3. Within the ionosphere between 90 and 200 km the plasma is partially ionized and collisions between neutral and charged particles play an important role. This region is characterized by the fact that the collision frequency for collisions between neutrals and ions is greater than that for collisions between neutrals and electrons. In other words, there exists a region, where the electrons are more tied to the magnetic field **B** than the ions. This situation has been characterized in the right hand part in Figure 1 by comparing the collision frequencies and the gyrofrequencies

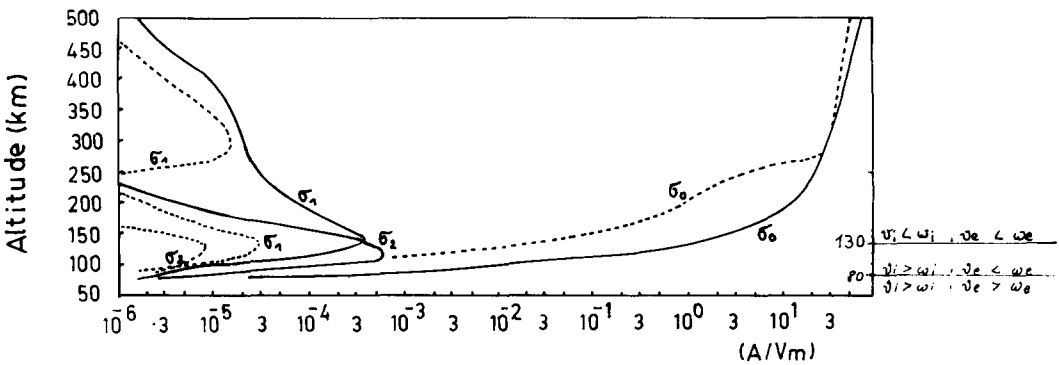

Fig. 1. Spitzer (σ_0), Pedersen (σ_1), and Hall (σ_2) conductivity in dependence on height for noon-time (full curve) and midnight (dashed curve).

of electrons and ions for different regions. Consequently, in this region charge accumulations and electric polarization fields **E** can be built up as a result of the different motions of the electrons and ions due to the different interactions with the neutral gas particles. This process has been called the 'atmospheric dynamo process'. It is the dominating mechanism producing ionospheric electric fields.

From Maxwell's equations of electrodynamics it follows that the distribution and generation of ionospheric electric fields by the atmospheric dynamo process can be described by

$$\begin{aligned} &\text{curl curl } \mathbf{E} + \mu_0 \frac{\partial}{\partial t} \boldsymbol{\sigma}(\mathbf{E} + \mathbf{v}_n \times \mathbf{B}_0) = 0\,, \\ &\text{div } \mathbf{j} = 0 = \text{div } (\boldsymbol{\sigma} \cdot \mathbf{E}) + \text{div } (\boldsymbol{\sigma} \cdot (\mathbf{v}_n \times \mathbf{B}_0)) \end{aligned} \tag{1.1}$$

($\mathbf{v}_n$ neutral wind, $\boldsymbol{\sigma}$ conductivity tensor, **j** current density) see Möhlmann and Wagner (1970). These equations describe quasistationary electric fields in the ionosphere. These fields propagate in a diffusion-like fashion out of the region of generation. Internal gravity waves and acoustic gravity waves can generate these time-dependent and relatively small-scale electric fields. The amplitude of these electric fields can be of the same order of magnitude as that of large-scale electric fields. These quasi-stationary processes will be a task for future investigations.

Since we are interested in large-scale global ionospheric electric fields during quiet conditions, we have to discuss electric fields with time scales of the order of 1 day. Taking into account that the diffusion length for an electric field within the ionosphere with a time scale of 1 day is of the order of 10 Earth radii, it can be understood that these electric fields have propagated around the Earth and reached a quasi-static state (curl $\mathbf{E} = 0$, $\mathbf{E} = -\text{grad } S$). Considering the accuracy of the available measurements of electric fields, it has been shown by Möhlmann (1971) that a quasi-static approximation is sufficient to describe large-scale ionospheric electric fields. With (1.1) follows

$$\text{div } (\boldsymbol{\sigma} \cdot \text{grad } S) = \text{div}(\boldsymbol{\sigma} \cdot (\mathbf{v}_n \times \mathbf{B}_0))\,, \tag{1.2}$$

(S = electrostatic potential).

From the so-called 'dynamo-equation' (1.2) it is obvious that the electric field **E** depends as well on the conductivity tensor $\boldsymbol{\sigma}$ of the ionospheric plasma as on the structure of the neutral winds $\mathbf{v}_n$.

The electrodynamic properties of the magnetospheric and ionospheric plasma are introduced in this equation through the tensor of electroconductivity

$$\boldsymbol{\sigma} = \begin{pmatrix} \sigma_0 & 0 & 0 \\ 0 & \sigma_1 & -\sigma_2 \\ 0 & \sigma_2 & \sigma_1 \end{pmatrix}. \tag{1.3}$$

Currents parallel to the magnetic field are proportional to the Spitzer-conductivity σ_0, and currents perpendicular to the magnetic field are dependent on the Pedersen-conductivity σ_1 and Hall-conductivity σ_2 (Akasofu and Chapman, 1972).

The tensor of electro-conductivity of the ionospheric plasma has been derived by the theory of plasma transport processes. The ionospheric plasma is tied to the magnetic main field of the Earth. This magnetic inhibition of free streaming is effective only in directions perpendicular to the magnetic field lines. Diffusion across the magnetic field leading to a weakening of the original inhibition is possible only because of collisions with neutral particles, which allow the charged particles to emigrate from one field line to the other. The resulting electro-conductivity must be described by a tensor. Figure 1 in the left part gives an estimation of the height dependence of the components of this tensor. The conductivity parallel to the magnetic field σ_0, the Spitzer-conductivity, the Pedersen-conductivity σ_1, and the Hall-conductivity σ_2 have been shown. From these material properties of the ionospheric plasma three interesting conclusions concerning electric fields and currents can be drawn:

- For large-scale electric fields and currents in the ionosphere there must be a 'quasi-short-circuit' along the magnetic field lines due to the dominating parallel conductivity. This means that for all geographical regions without the magnetic equator and its neighbourhood the electric fields have only a very weak height dependence.
- Essential currents perpendicular to the magnetic main field can flow only in a height region between 100 and 200 km.
- The ionospheric conductivity distribution shows strong gradients of the perpendicular components at about 100 km and at about 130 km, which may have an importance for the generation of large-scale ionospheric electric fields (see below).

Equation (1.2) also shows that the electric field depends on the generating neutral winds. Therefore, it is necessary to discuss the dynamics of the neutral gas.

The energy driving the neutral wind systems results from the absorption of solar radiation within the atmosphere. Speaking generally, there are two main regions of absorption, i.e. two heat sources driving neutral wind systems. One heat source exists in the ozone-layer, and in the watervapor-layer, both below 85 km. The neutral gas motions produced by absorption of the solar radiation within these layers can be described by the tidal theory see Lindzen (1971), Wagner (1968), Chapman and

Lindzen (1970), Volland and Mayr (1974), Volland (1974a, b). In the tidal theory it has been shown that a lot of different wind modes may be generated, but most of these cannot propagate to greater heights than 100 km because they are absorbed and dissipated near the turbopause. Only modes with great vertical wavelengths are able to penetrate through this region. In many cases also the amplitudes of these wind modes are diminished by absorption and dissipation.

Solar radiation in the EUV- and UV-part is absorbed by ionization processes and dissociation processes of molecular oxygen and molecular nitrogen well above 100 km. The center of this absorption regions exists in about 150 km. This heat source has been observed first by neutral gas density measurements showing the existence of a well pronounced diurnal bulge (see Jacchia, 1965), which may be detected in different altitudes. This heat source creates thermospheric wind systems. These wind systems have been investigated by Kohl and King (1967), Blum and Harris (1972, 1975a, b), Hines (1965), Geisler (1966, 1967), Lindzen (1967).

The amplitude and the phase of this thermospheric wind has been calculated in dependence on latitude, longitude and altitude by Volland and Mayr (1973). The results are shown in Figure 2. Mathematically, it is possible to describe this thermospheric wind in a good approximation by a modified Hough-function (1, −2)*. Since the tidal mode (1, −2) can be generated at *F*-region heights too (see

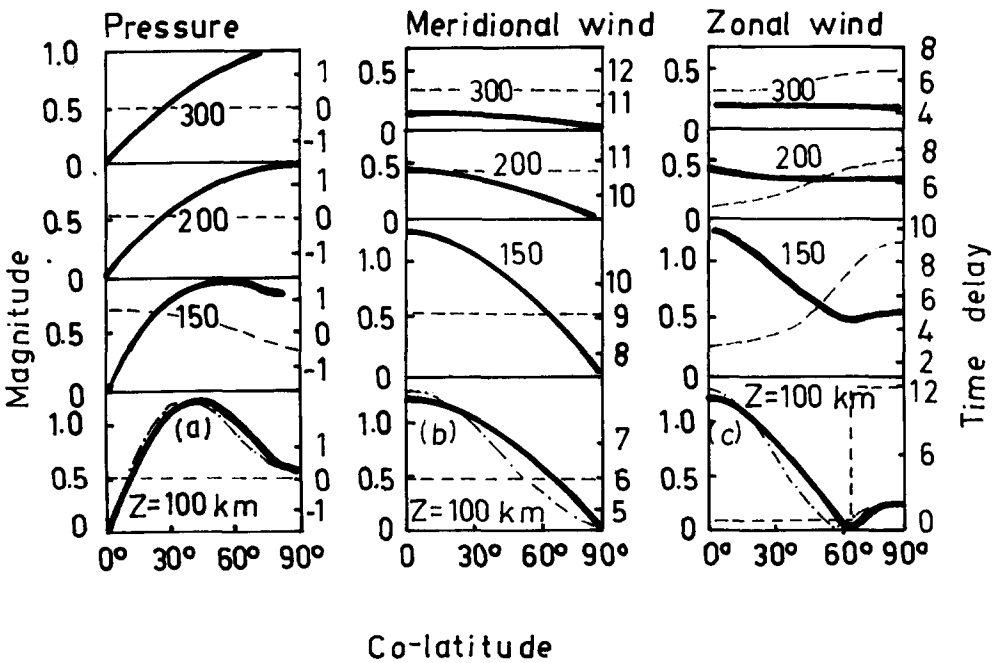

Fig. 2. Relative wave amplitudes of the (1, −2)-tidal mode pressure and wind components in dependence on colatitude after Volland and Mayr (1973).

* The 1, −2 tidal mode corresponds to the (1, −1) mode in the older literature on tidal modes.

Volland, 1976a), it is possible to use the Hough-function (1, −2) with a modified height-dependence for the description of one main wind component for the whole ionosphere.

Knowing the main properties of the electric conductivity and the neutral winds, it is possible to draw some conclusions about the effectiveness of the dynamo process. The influence of both the electric conductivity of the ionospheric plasma and the neutral winds on the generation of electric fields is described by (1, 2).

As can be seen from the right-hand part of Figure 1, the region, where electric fields may be produced, extends from about 100 km up to about 150 km. The perpendicular conductivities have their maxima in the region between 100 km and 125 km. In the lower parts of this region, tidal wind modes may be dominating, in the upper part, thermospheric winds may play an important role. Three principal conclusions for the electric fields may be drawn from the general situation described in Figure 1:

– Let us investigate that altitude range, where the perpendicular conductivities have their maxima. Different neutral wind modes may exist within this region. Each wind mode having a vertical wave-length smaller than the altitude range of high conductivities will create electric fields changing rapidly (in their direction) and therefore being cancelled out due to the high parallel conductivity through the whole altitude range. All these winds will result at most in very small electric fields. In other words, only wind modes with a vertical wave-length > 20 km may lead to observable field strengths. This statement is independent of the amplitude of the wind modes, i.e. if we have a neutral wind composed of one wind mode with high amplitude and small vertical wave-length, and another wind mode with much smaller amplitude, but a very large vertical wave-length, only the second wind mode will be effective in generating electric fields, and therefore, will be interesting for the comparison of measured neutral winds, and measured electric fields.

– Since only the composed action of electric conductivity, and winds determines the amplitude of the resulting electric field, not only the E-region with high conductivity, but lower wind velocity, but also the F-region with lower conductivity but higher wind amplitudes may be a region suitable for the generation of ionospheric electric fields. For a long time only the E-region dynamo has been taken into consideration. But Rishbeth (1971), Matuura (1974) and Volland (1976) suggested that the F-layer-dynamo may give considerable contributions. This has, at least for low latitudes, proved by Heelis *et al.* (1974) (see Figure 3). The dotted curve shows averaged vertical ion velocity measurements from Jicamarca, the full curve gives theoretically computed values using only the E-layer-dynamo and the dashed one values from E- and F-layer dynamo-electric fields; all data for 300 km altitude. Reproducing the measurement is only possible introducing the F-layer-dynamo.

– Physically, it is clear that regions with steep gradients of electro-conductivities are those of strong charge accumulations. The strongest spatial dependence of the fields in the dynamo-equation (1.2) is that of the height-dependence of the electro-conductivities. Therefore, the dominating charge accumulations are connected with

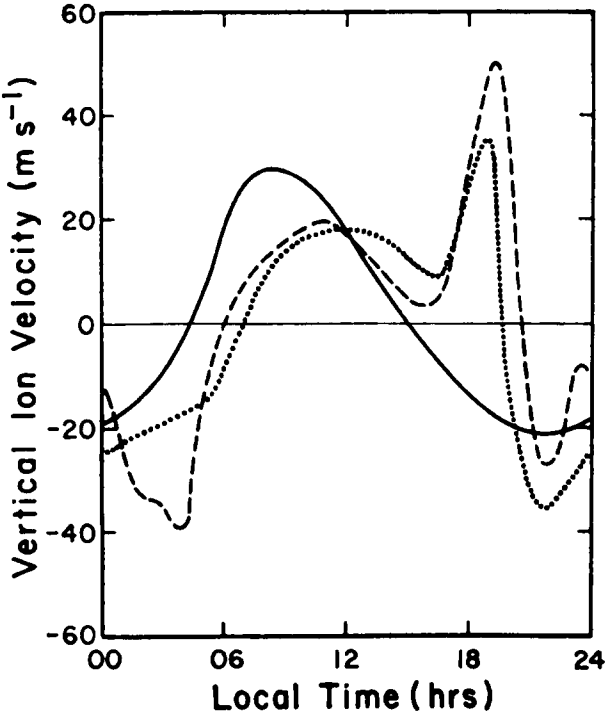

Fig. 3. Vertical drift velocity, average from 1968–69 Jicamarca observations of Woodmann (1970) around equinox (. . . . . .) compared with vertical ion velocity at 300 km above the equator computed theoretically from tidal E-region electric field only (——) and tidal E-region and F-region polarization fields (– – –). (After Heelis *et al.*, 1974).

the vertical σ-gradients. In general, the effectivity of the horizontal changes of $\mathbf{v}_n$ and σ in generating charge accumulations is smaller by one order of magnitude or more, since the connected characteristical lengths are smaller by the same order than the characteristical length for the vertical σ changes. An exception for this discussion are sunrise and sunset conditions in the equatorial electrojet region.

Electric fields may be generated in different regions but due to the domination of the parallel conductivity they are always superposing and giving the same potential along the line of force. This means, that the large-scale ionospheric electric field does not change essentially with height.

Electric currents are driven by this field mainly in the region of highest conductivity, i.e. that currents perpendicular to the magnetic field mainly flow in the region between 100 and 150 km. This agrees with the results of many rocket measurements.

For high latitudes many estimations have shown that the atmospheric dynamo process is not effective enough to explain the measured electric fields during quiet conditions. To produce these electric fields the winds should have amplitudes of 150 m s^{-1} to 1500 m s^{-1}. Such velocities do not exist in the atmospheric dynamo layer during quiet conditions. Therefore, the ionospheric electric fields at higher latitudes must be due to magnetospheric dynamo processes and connected with the

field-aligned current layers. Detailed measurements of the (spatial) structure and distribution of these coupling currents seem to be the key for the progress in understanding of large-scale magnetospheric electric fields and their 'generators'. First results in this direction have been deduced from TRIAD-measurements (Iijima and Potemra, 1976), a review see Akasofu (1977) or Wagner (1977, 1978).

2. Regular Variations of Electric Field and Currents and Related Magnetic Variations

2.1. Contribution of different sources to the *Sq* variations and plasmaspheric electric fields

During recent years there has been an intensive discussion of the question how much of the *Sq*-fields originates from electric fields and currents generated in the ionosphere and how much from the distant magnetosphere.

Olson (1970) estimated the contributions of the magnetopause currents and of the tail currents to the *Sq*-variations. Field-aligned currents of the DRP current system were shown to give a noticeable contribution to the *Sq*-variations in medium latitudes as has been shown by Fukushima and Kamide (1973) and Bhargava and Jacob (1971). For the *Sq*-variations in low latitudes Sarabhai and Nair (1969) and Kane (1971) found a pronounced correlation with parameters of the solar wind. Similar results have been found by Nishida (1971), but these have been criticized by Matsushita and Balsley (1972).

These results led Matsushita (1971) to the hypothesis that also the convection within the plasmasphere and therefore the *Sq*-vortices are a by-product of the main convection system in the tail, driven by energy from the solar wind. Theoretically a similar – but not identical – hypothesis is given in the paper of Glushakov and Samochin (1974). On the basis of experimental data this hypothesis of the influence of high-latitudinal electric fields on the ionosphere in medium latitudes has been checked by Stening (1973), Carpenter and Kirchhoff (1975), Matsushita (1975), and others. On the other hand, Lyatzkij and Maltzev (1975) showed theoretically that *Sq*-like equivalent current systems also result from a pair of field-aligned current sheets near the polar cap, if there exist downward flowing currents in the morning and upward currents in the evening sector. Mishin *et al.* (1975) showed that field-aligned currents and the various possible convective systems in the distant magnetosphere may result in noticeable contributions to the *Sq*-current system.

Since so many different sources may contribute to the electric fields, currents and geomagnetic *Sq*-variations in medium latitudes, it is necessary to estimate whether the sources from the distant magnetosphere (or the high-latitudinal ionosphere) or the atmospheric dynamo process give the overwhelming contribution. This problem has been discussed by several authors.

Matsushita (1975) showed that day-time variations of the electric field in high latitudes are not correlated noticeably with fields in medium latitudes, so that there is

no reason to assume that the high-latitudinal electric fields penetrate into the plasmasphere during undisturbed conditions. An analogical conclusion follows from the investigations of Gringauz *et al.* (1977) about the noon-bulge of the plasmapause.

Carpenter (1978) investigated whistler-data and showed that the data strongly support the conception that the electric fields observed inside the plasmasphere are due to ionospheric dynamo processes. The noon-midnight asymmetry (or noon-bulge) of the plasmasphere appears to be a consequence of these fields.

Vertlib and Wagner (1977) showed that the geographical latitude is much more suitable for the description of seasonal variations of the Sq-current system than the geomagnetic one and concluded that only a minor part (10 to 15%) of the Sq-current system is due to magnetospheric contribution (see also Wagner, 1971).

So we concluded that the main source of electric fields and currents in the quiet day-side plasmasphere and of magnetic variations in the quiet mid-latitudinal ionosphere is the atmospheric dynamo. Magnetic variations due to the various magnetospheric processes give a contribution up to 20%, depending very much on the location of the observatory and on activity (see review Heppner (1972, 1977), Stern (1977), Mishin *et al.* (1979)). During recent years daily variations of ionospheric electric fields have been determined from ion drift velocity measurements.

$$\mathbf{v}_D = (\mathbf{E} \times \mathbf{B})/B^2 \tag{2.1}$$

by incoherent scatter stations in medium latitudes. Based on such measurements an averaged gross distribution in dependence on (apex) latitude for the electrostatic potential has been calculated by Richmond (1976) as a series of spherical harmonics up to $n = 6$ (see Figure 4a). This global map is an important step towards a better understanding of the processes. The two extrema at 07:00 LT and 20:00 LT coincide

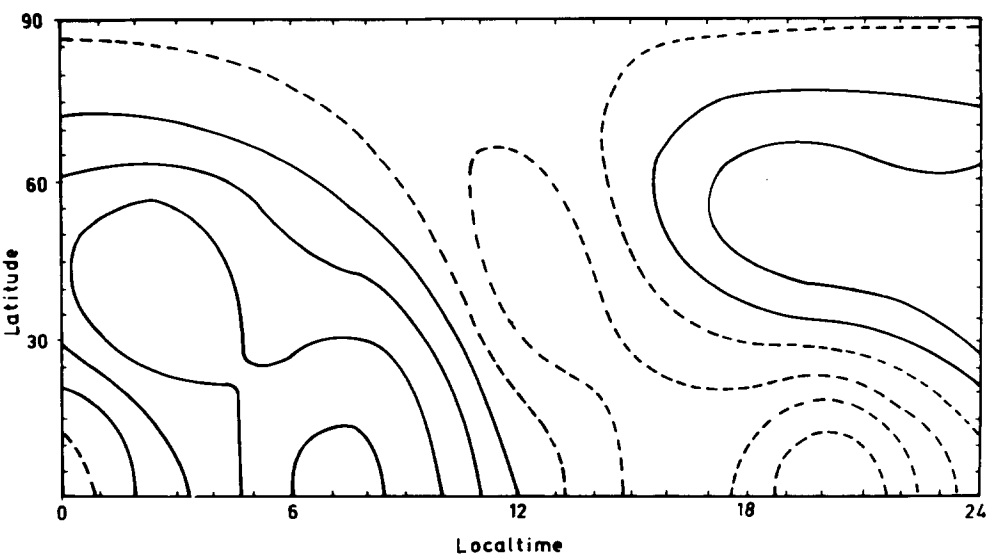

Fig. 4a. Global distribution of the electrostatic potential in ionospheric heights (Richmond, 1976) (Distance of isolines − 1 kV).

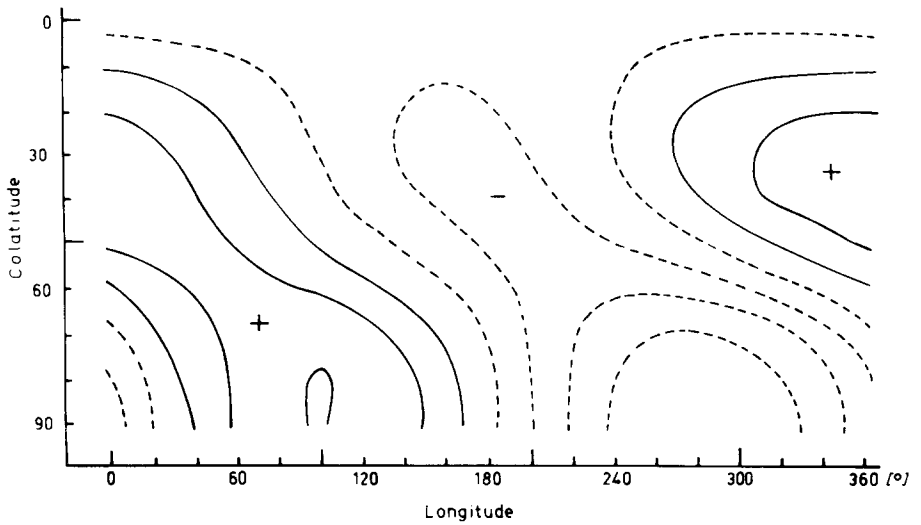

Fig. 4b. Global distribution of the electrostatic potential produced by a superposition of the tidal modes (1, −2) and (1, 1) and a zonal component after Möhlmann (1977).

with the ends of the high conducting equatorial electrojet region thus illustrating the importance of conductivity gradients for the generation of polarization fields (see Section 1).

Measurements of the daily variations of the ion drift velocity for equinox (averages and a special day) are shown for Saint-Santin in Figure 5 (from Blanc and Amayenc, 1976). Such measurements give a good possibility to testify theoretical calculations. Some preliminary investigations have shown that a regular seasonal variation of the electric field in medium latitudes seems to exist, but so far the results are sparse. So, we have to state that for the global electric fields we know only the gross features. The only possibility to investigate more detailed regular variations (e.g. seasonal) offer magnetic measurements.

2.2. Longitudinal (UT) and seasonal variations of *Sq* current systems

Worldwide measurements of the mean solar daily quiet geomagnetic variations show that in a first approximation these variations depend on local time t on latitude φ. In a second approximation one finds seasonal dependencies of the *Sq*-variations due to the declination of the Earth's rotation axis towards the ecliptic plane and longitudinal (λ) or universal time (T; UT) variations due to the non-coincidence of the magnetic axis with the rotation axis of the Earth. Results of this kind of investigations are especially interesting because they show for the first time that the symmetrical dynamo model is insufficient and plasmaspheric field-aligned currents play an important role.

2.2.1. *Longitudinal or UT-Variations of the Sq-field*

Watching the *Sq*-field from the Sun one sees regular periodical variations with universal time T as an effect of the rotation of the magnetic axis. Since $T = t - \lambda$,

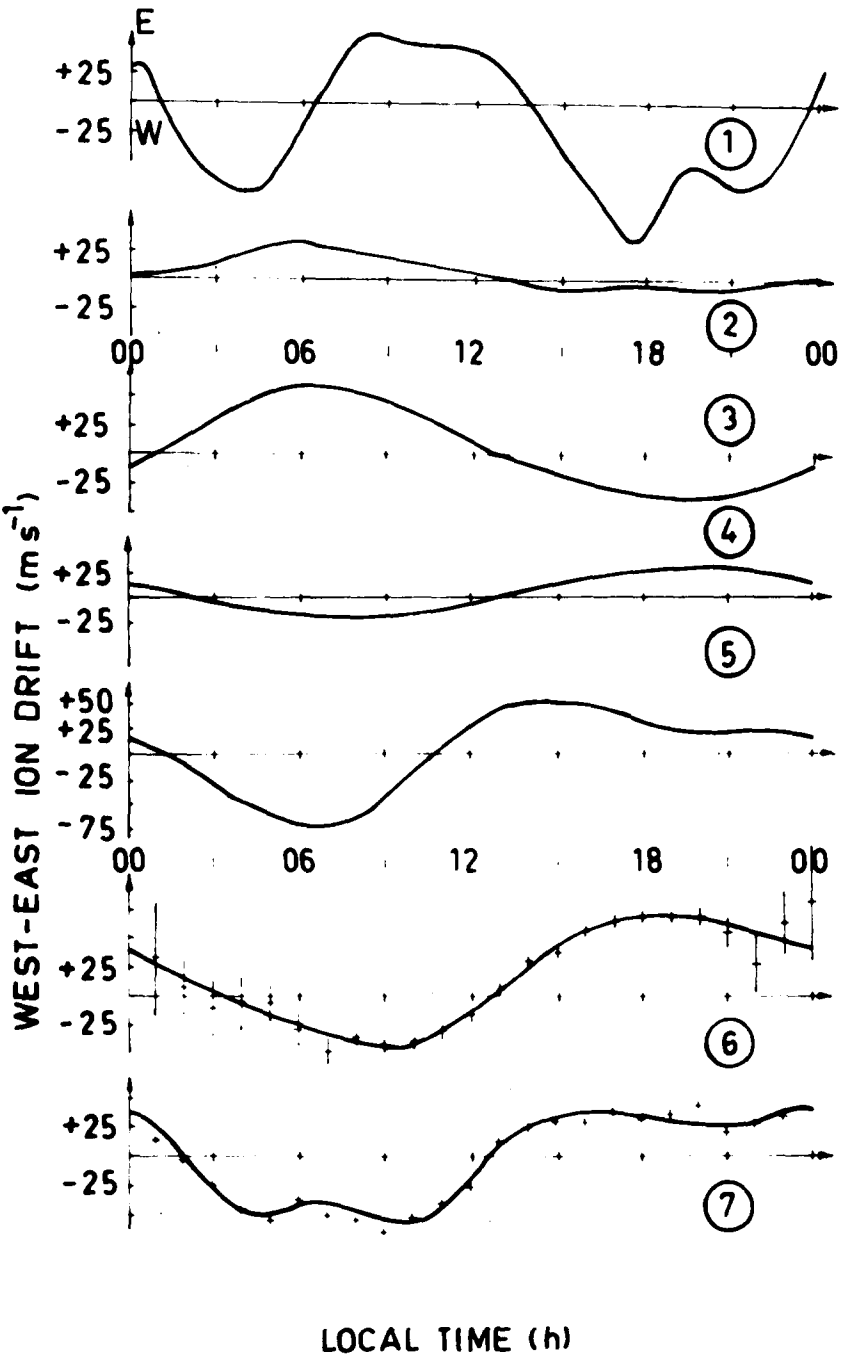

Fig. 5. Comparison between theoretical ion drift values computed from different dynamo models and experimental results obtained at Saint-Santin: (1) Stening (1974) dynamo model, (2) Matsushita/Tarpley (1970) dynamo model, (3) Matsushita (1971) plasmaspheric model, (4) Möhlmann's global model (1977), (5) Schäfer (1978) threedimensional model, (6) experimental data March 19–20, 1974, and (7) 'median' model taken from equinox and winter results after Blanc and Amayenc (1976).

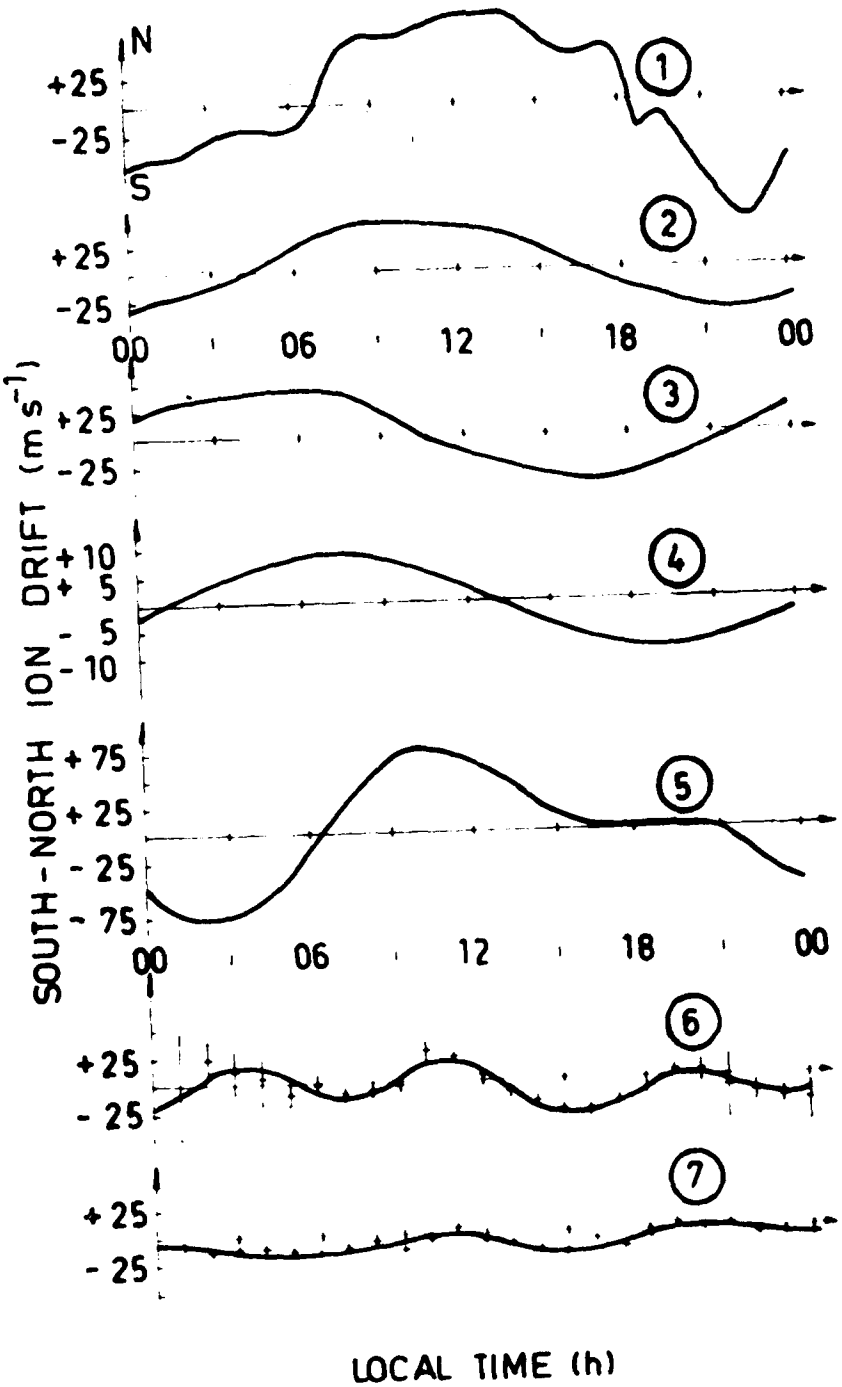

Fig. 5 (continued).

these variations may be described analytically by terms depending on the geographic longitude λ.

Two different methods have been used to analyse the UT-dependence of the *Sq*-field; using the spheric harmonic analysis the total current and the positions of the foci of the vortices of the equivalent current system have been calculated from a global data material for different UT-values. In this manner the UT-dependence of the total current and the position of the foci has been calculated by Hasegawa (1936, 1937, 1938, 1950), Price and Wilkins (1963), and Benkova (1941) for the material of the Second International Polar Year 1932/33. The main results (see Figure 6) were:

(a) For the foci there exists a regular variation in latitude with UT with an amplitude up to 15–20°.

(b) The co-latitude of the focus has a maximum between 15:00–18:00 UT in the northern hemisphere as well as in the southern one.

(c) The variation of the total current with UT was found to be in antiphase on both hemispheres by Hasegawa, whereas from Benkova's data it was found by Mishin and Bazarzhapov to be in phase (see Mishin, 1976).

Nowadays the methods have been improved and the global coverage of the data as well as its accuracy is better. Using the spherical harmonics analysis combined with the method of the election of optimal spectra of the approximating functions developed by Mishin and Bazarzhapov, these authors investigated the UT-variation for the IGY-period (see Mishin *et al.*, 1971; Mishin, 1976). Calculations have been performed for annual mean values but also for different seasons. Figure 7 shows detailed results for different seasons (equinox, northern winter, northern summer).

The upper part of Figure 7 gives the total current, the lower one the position of the foci in dependence on co-latitude and local time t for different UT-values. Without taking into account the peculiarities of the different seasons, the following general results are obvious;

(a) The co-latitude of the foci shows a UT-variation, which occurs in phase on both hemispheres. On the northern hemisphere the co-latitude has its minimum around 05:00 UT and its maximum around 17:00 UT. The amplitude of the latitudinal variation is smaller on the northern hemisphere than on the southern one.

(b) The longitude of the focus also depends on UT in such a manner that the focus position describes a closed orbit during one day. On the northern hemisphere the focus moves anticlockwise, on the southern hemisphere clockwise.

(c) The total current shows a UT-variation of 30–50% of the daily mean value, the variations are greater on the southern hemisphere than on the northern one. The variations are in phase on both hemispheres with a maximum at 12:00–18:00 UT.

These results, in principle, are valid for all seasons. Differences occur due to changes in the daily mean value and due to the superposition of an annual and semi-annual variation. Figure 7 shows the maximum of the total current for northern winter at 15:00–18:00 UT and for northern summer at 12:00–15:00 UT. The amplitude of the UT-variation of the northern total current in winter is twice that found during summer. Neglecting smaller details one can state that the UT-variation

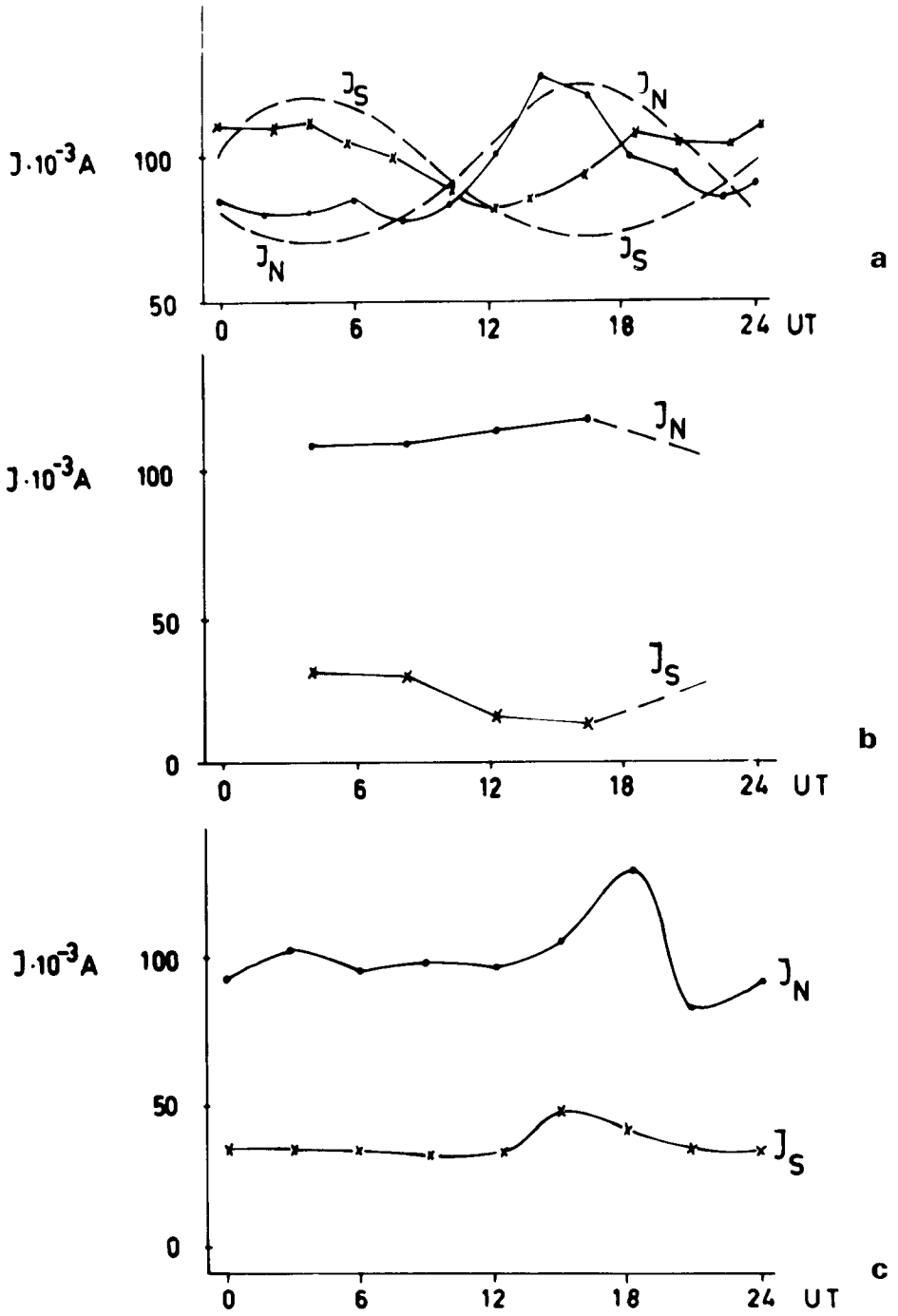

Fig. 6. UT-variation of the total current within the northern (I_N) and southern (I_S) *Sq*-vortex. (a) Hasegawa, Ota (1950); dashed lines – theoretical results from Nagata and Sugiura (1948). (b) Price and Wilkins (1963). (c) Mishin (1976) based on data from Benkova (1941).

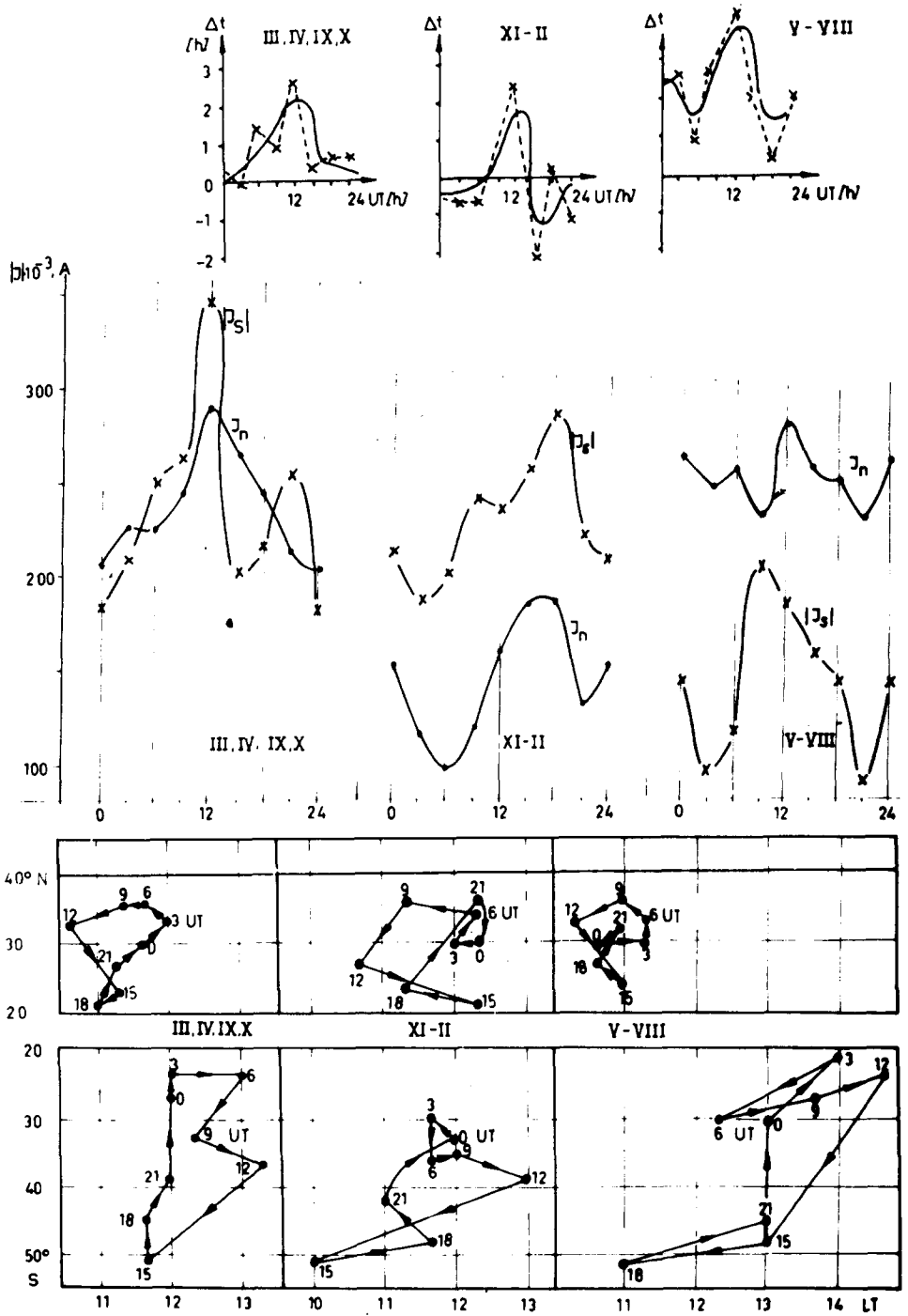

Fig. 7. UT-variation of the shift of foci Δt_f, the total current and the position of the foci of the northern and southern *Sq*-vortex in dependence on season, IGY-data.

of the focus latitude does not differ very much from season to season. The UT-variation of the focus longitude resp. the local time of the focus is much more complicated. At the top of Figure 7 the time-difference Δt_f of the occurrence of the current density maxima in the northern and southern hemisphere has been drawn in dependence on universal time (UT) and season. The maximum always occurs at 12:00 UT. The average $\overline{\Delta t_f}$ is always positive, i.e. the maximum in the northern hemisphere always occurs earlier than that of the southern hemisphere.

The second method to analyse the UT-variations of the *Sq*-field was developed by Mishin and Nemzova (1966), Nemzova (1966), and Mishin (1976). This method separates the UT- from the LT-variation of the *Sq*-field for the magnetic field strength $F = \sqrt{X^2 + Y^2 + Z^2}$ or the horizontal intensity $H = \sqrt{X^2 + Y^2}$ (X, Y, Z magnetic components of the *Sq*-field): Let us write as usually

$$F(t, T, \varphi) = \sum_{m=0} [\alpha_m(T, \varphi) \cos mt + \beta_m(T, \varphi) \sin mt] \tag{2.2}$$

with

$$\alpha_m(T, \varphi) = \sum_{k=0} (a_{k,m} \cos kT + b_{k,m} \sin kT)\,,$$

$$\beta_m(T, \varphi) = \sum_{k=0} (c_{k,m} \cos kT + d_{k,m} \sin kT)\,. \tag{2.3}$$

Taking into consideration only first-order terms one may write

$$\begin{aligned} F(t, T, \varphi) &= a_0 + a \cos T + b \sin T + A' \cos t + B' \sin t + F' = \\ &= a_{0.0} + a_{1.0} \cos T + b_{1.0} \sin T + a_{0.1} \cos t + c_{0.1} \sin t + F' \end{aligned} \tag{2.4}$$

with F' describing smaller and irregular contributions from higher harmonics. From (2.4) follows:

$$\begin{aligned} &F(t, T, \varphi) = F_L + F_u + F', \\ &F_L = A' \cos t + B' \sin t = R \cos (t - \psi) \quad \text{(LT-component)}, \\ &F_u = a \cos T + b \sin T = r \cos (T - \gamma) \quad \text{(UT-component)}. \end{aligned} \tag{2.5}$$

If one has a representation of the *Sq*-variation from many observatories in the form

$$\begin{aligned} F &= \sum_{n=0} (A_n \cos nT + B_n \sin nT) = \\ &= a_0(\varphi) + A_1 \cos T + B_1 \sin T \end{aligned} \tag{2.6}$$

these data may be used to calculate the coefficients of the LT- and UT-component F_L and F_u: Introducing $t = T + \lambda$ (λ = geographic longitude) into (2.4) it follows from (2.6)

$$\begin{aligned} A_1(\varphi, \lambda) &= a(\varphi) + A'(\varphi) \cos \lambda + B'(\varphi) \sin \lambda\,, \\ B_1(\varphi, \lambda) &= b(\varphi) - A'(\varphi) \sin \lambda + B'(\varphi) \cos \lambda\,. \end{aligned} \tag{2.7}$$

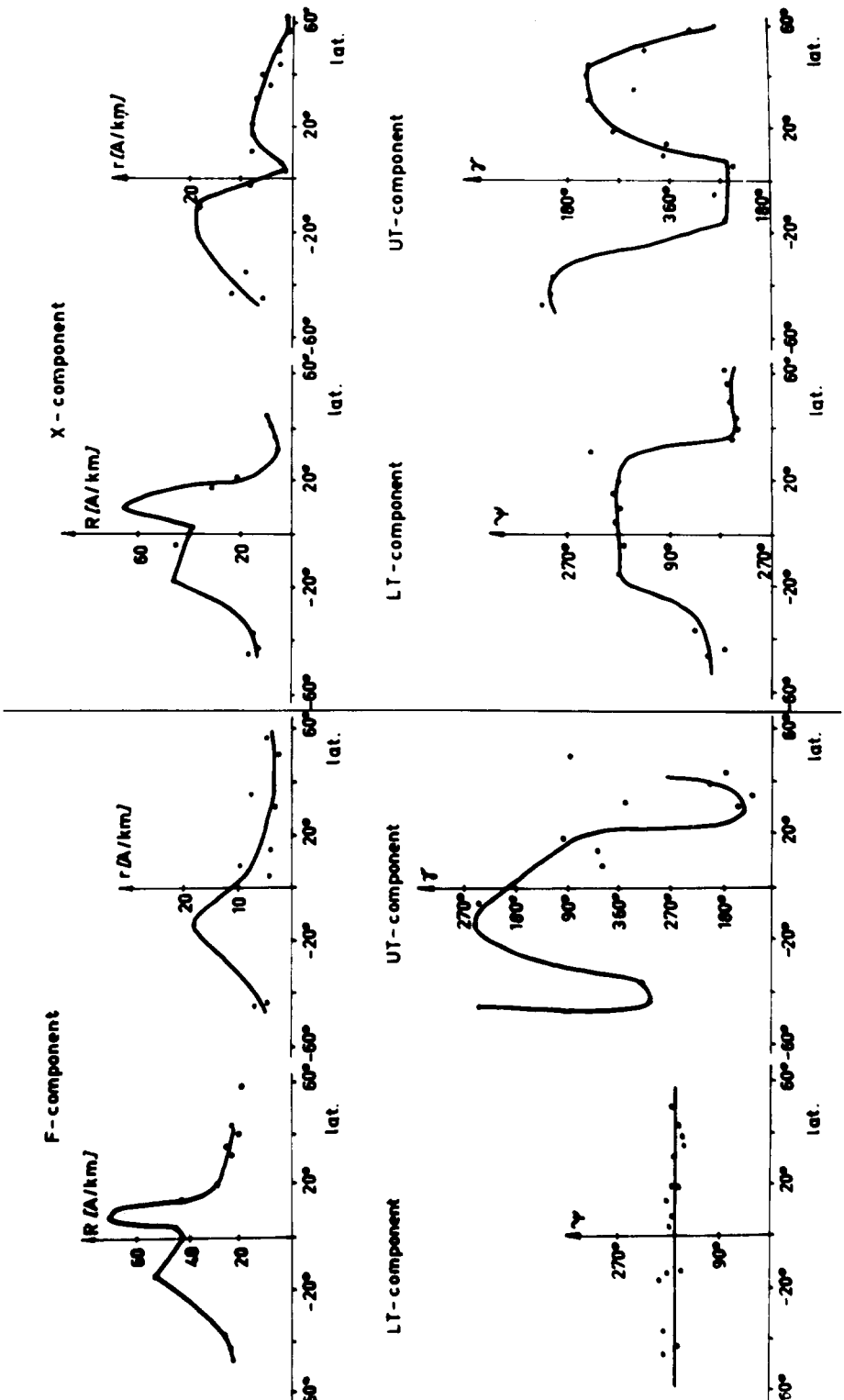

Fig. 8. Parameters of the local time (LT) and universal time (UT) dependencies of the *Sq*-X-component and the total field-strength *F*, equinox, IGY-data.

Using this system of equations and having descriptions of F by (2.6) for observatories at the same latitude φ and different longitudes λ, it is possible to calculate a and b as well as A' and B' as a function of latitude, i.e. to separate the LT- and UT-dependencies (see (2.5)). The results have been drawn in Figure 8, showing the amplitudes R, r and phases ψ, γ of the functions F_L and F_U in dependence on latitude φ for equinoces of the IGY for the F- and X-components. The LT-part F_L shows, in principle, the well-known behaviour. According to Figure 8 the amplitude of the UT-component is 2–8nT in medium northern latitudes but much greater on the southern hemisphere. On average, the UT-variation reaches 20–40% of the daily mean value. The phases for F are much more difficult to describe, because they consist of different parts. For the X-component the phases in the northern and southern hemisphere correspond very well. From these data Mishin (1976) assuming $F \approx H \approx (2\pi/0.6) I_{[A/m]}$ has estimated the current density and the total current in the northern and southern vortex. He found: The total current changes periodically with UT, having an amplitude of 50–100 kÅ and a maximum in the period 12:00–18:00 UT. The UT-variations occur in phase on both hemispheres. The amplitude is greater at the southern hemisphere. These results totally coincide with those described above and given in Figure 7. Additional investigations for the different seasons give the same results. So, two independent methods led to the same results for the UT-variations. Concerning the foci these new results coincide with the older ones (see above). The latitudes of both foci shift from north to south from before-noon to the afternoon (see Figure 7). Mishin (1976) has explained this variation of the focus latitude as a direct result of the precession of the magnetic axis around the rotation axis, i.e. a consequence of the daily variation of the dipole.

This idea is also supported by the result that the UT-variation of the foci shows only a small seasonal variation. In order to explain the UT-characteristics of the total current (in phase variation on both hemispheres, greater amplitudes on the southern one) it is necessary to examine the influence of the precession of the magnetic axis on the electric conductivity.

2.2.2. *UT-Variations of the Electric Conductivity-Tensor*

The Pedersen-conductivity σ_1 and Hall-conductivity σ_2 can be calculated by

$$\sigma_1 = \frac{e^2 n_e}{m_e} \frac{\nu_e}{\nu_e^2 + \omega_e^2} + \frac{e^2 n_e}{m_i} \frac{\nu_i}{\nu_i^2 + \omega_i^2},$$

$$\sigma_2 = \frac{e^2 n_e}{m_e} \frac{\omega_e}{\nu_e^2 + \omega_e^2} - \frac{e^2 n_e}{m_i} \frac{\omega_i}{\nu_i^2 + \omega_i^2}. \tag{2.8}$$

Knowing the collision frequencies ν_e, ν_i, the electron density n_e and the main geomagnetic field in dependence on latitude and longitude, it is possible to calculate the gyrofrequencies ω_e, ω_i and σ_1 σ_2. The longitudinal variation of the main magnetic field results in a UT-variation of the conductivity. Adam *et al.* (1964) calculated the magnitude of the main field in 160 km height in dependence on

latitude and longitude (see Figure 9a). They found that the amplitude of the longitudinal variation:

(a) reaches 20–30% of the average latitudinal value;

(b) is stronger by a factor 3–4 on the southern hemisphere than on the northern one;

(c) shows a 360° periodicity with a maximum at $\lambda = 120°$ on the southern hemisphere; and

(d) shows a 180° periodicity with two maxima at $\lambda = 120°$ and $\lambda = 270°$ with the same magnitude on the northern hemisphere.

The UT- or longitudinal variation of the main magnetic field is presented in another form in Figure 9b (see Cole and Thomas, 1968). Starting at an altitude of 300 km in one hemisphere, the value of B at the corresponding geomagnetic conjugate place at 300 km altitude has been computed and contours of equal

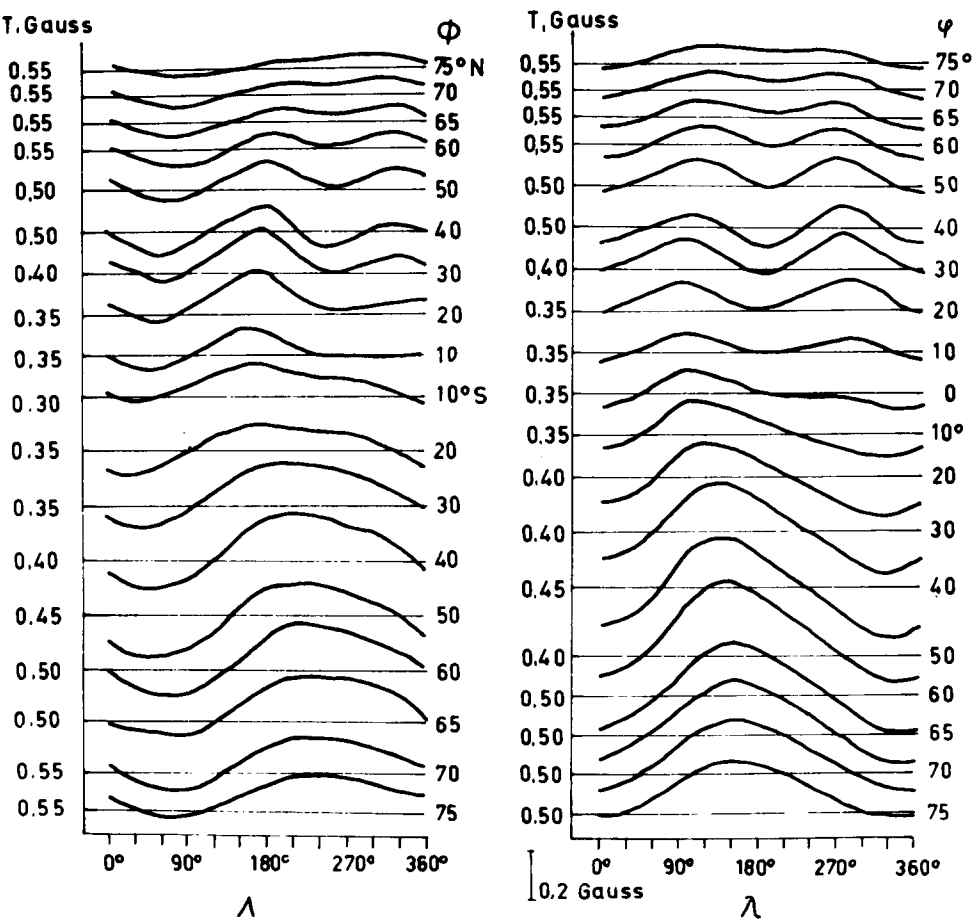

Fig. 9a. Total intensity of the main magnetic field in 100 km altitude in dependence on geographic and geomagnetic coordinates after Adam, Benkova and Orlov (1964).

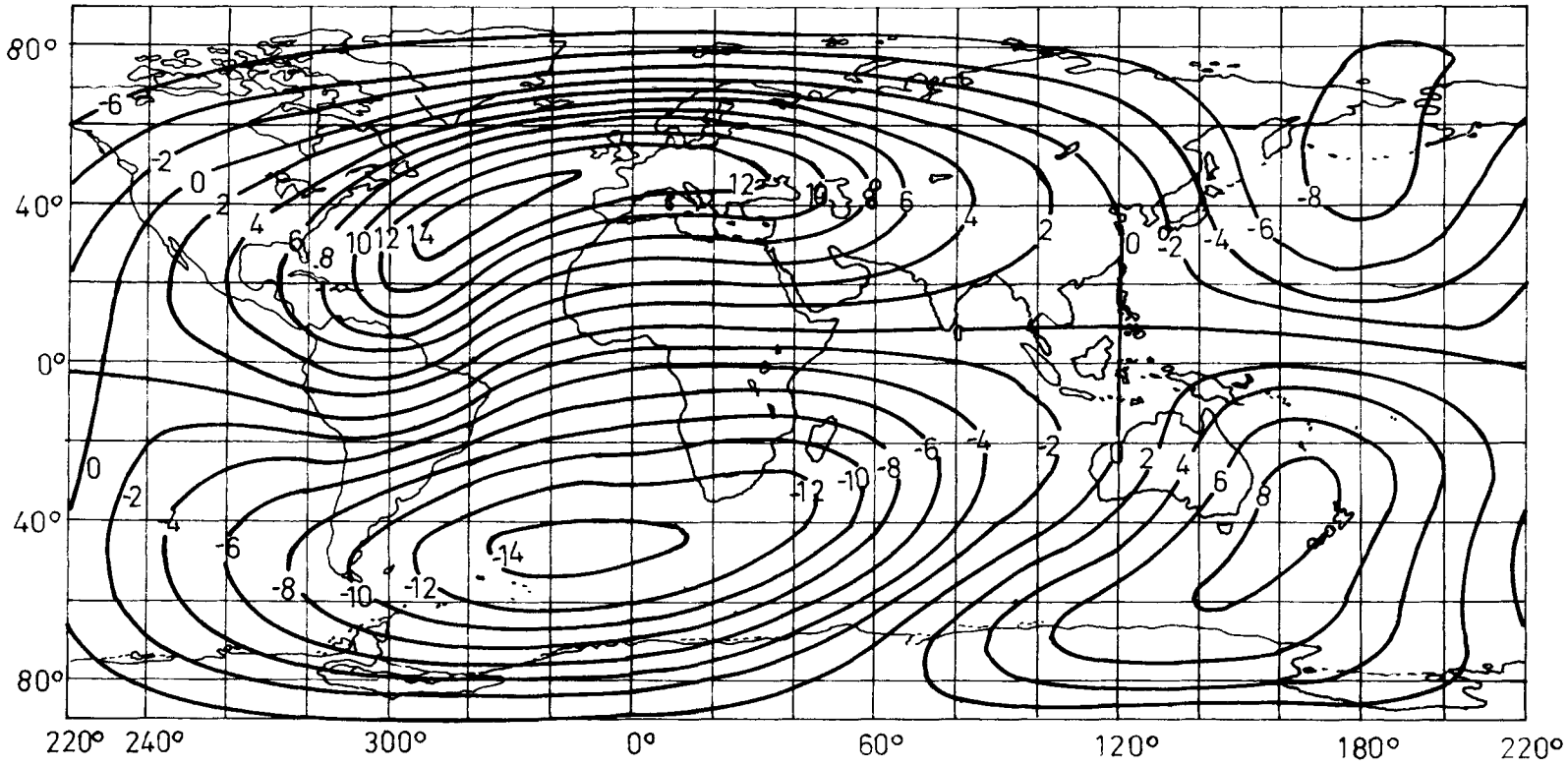

Fig. 9b. Maps of the difference in geomagnetic field at conjugated areas after Cole and Thomas (1968).

differences of B have been drawn B (North) – B (South) on the northern and B (South) – B (North) on the southern hemisphere.

Using the data from Figure 9a and the electron density data from Izmiran (1958, 1963), Nemtzova and Mishin (1970), and Mishin and Erushenkov (1966) calculated the electric conductivity in dependence on local time, universal time and latitude. Since the data will be used here to interpret UT-variations of equivalent currents and since these currents perpendicular to the magnetic field will mainly flow in the height region 90–150 km (see Figure 1), we will concentrate on the UT-variation of the height-integrated conductivities

$$\Sigma_1 = \int_{90}^{150} \sigma_1 \, \mathrm{d}h \quad \text{and} \quad \Sigma_2 = \int_{90}^{150} \sigma_2 \, \mathrm{d}h$$

as well as the Cowling-conductivity

$$\Sigma_3 = \Sigma_1 + (\Sigma_2)^2 / \Sigma_1 \, .$$

The highest conductivity values occur around local noon. Due to the longitudinal variation of the main field, the UT-variations of the local noon values show 24- and 12-hour periodicities with amplitudes and phases depending on latitude; these variations may be described by

$$\Sigma_k = \sum_{m=0}^{2} r_{k,m} \cos (mT - \alpha_{k,m}), \qquad k = 1, 2, 3 \, . \tag{2.9}$$

The results are drawn in Figure 10. It is obvious, that on the northern hemisphere UT-variations of the conductivity are rather small and practically absent especially for Σ_3. On the southern hemisphere the amplitudes are much higher, especially in 20–30° latitude; maxima for all Σ_k and for all southern latitudes occur about 13:00 UT ($\alpha_k = 200°$). On average, the maximal amplitude of the UT-variation is about 30% of the daily mean value. For estimations values $\bar{\Sigma}_k$ averaged across the vortex area of $\bar{\Sigma}_3 : \bar{\Sigma}_2 : \bar{\Sigma}_1 = 5 : 2 : 1$ may be used. The next step (see below) is to investigate whether this increase of the conductivity on the southern hemisphere with a maximum at 13 : 00 UT is able to produce the UT-variation of the total current on both hemispheres.

2.2.3. *Seasonal Variations of the Sq-Field*

It has been known for a long time (see Chapman and Bartels, 1940; last review Kane, 1976) that there exists an annual variation of the Sq-field, but some details and also the ratio $I_{\text{summer}}/I_{\text{winter}}$ have been controversery. During the last decade it has been shown that besides the annual variation there also exists a semi-annual one (see Wiese, 1951; Matsushita and Maeda, 1965; Mishin *et al.*, 1966; Wagner, 1968, 1969; Vertlib and Wagner, 1970, 1977). As for the UT-variations, in this case two different methods have been used, too.

Vertlib and Wagner (1970, 1977) studied the annual and seasonal variations and their dependence on latitude for 22 stations. Quiet days have been selected for the

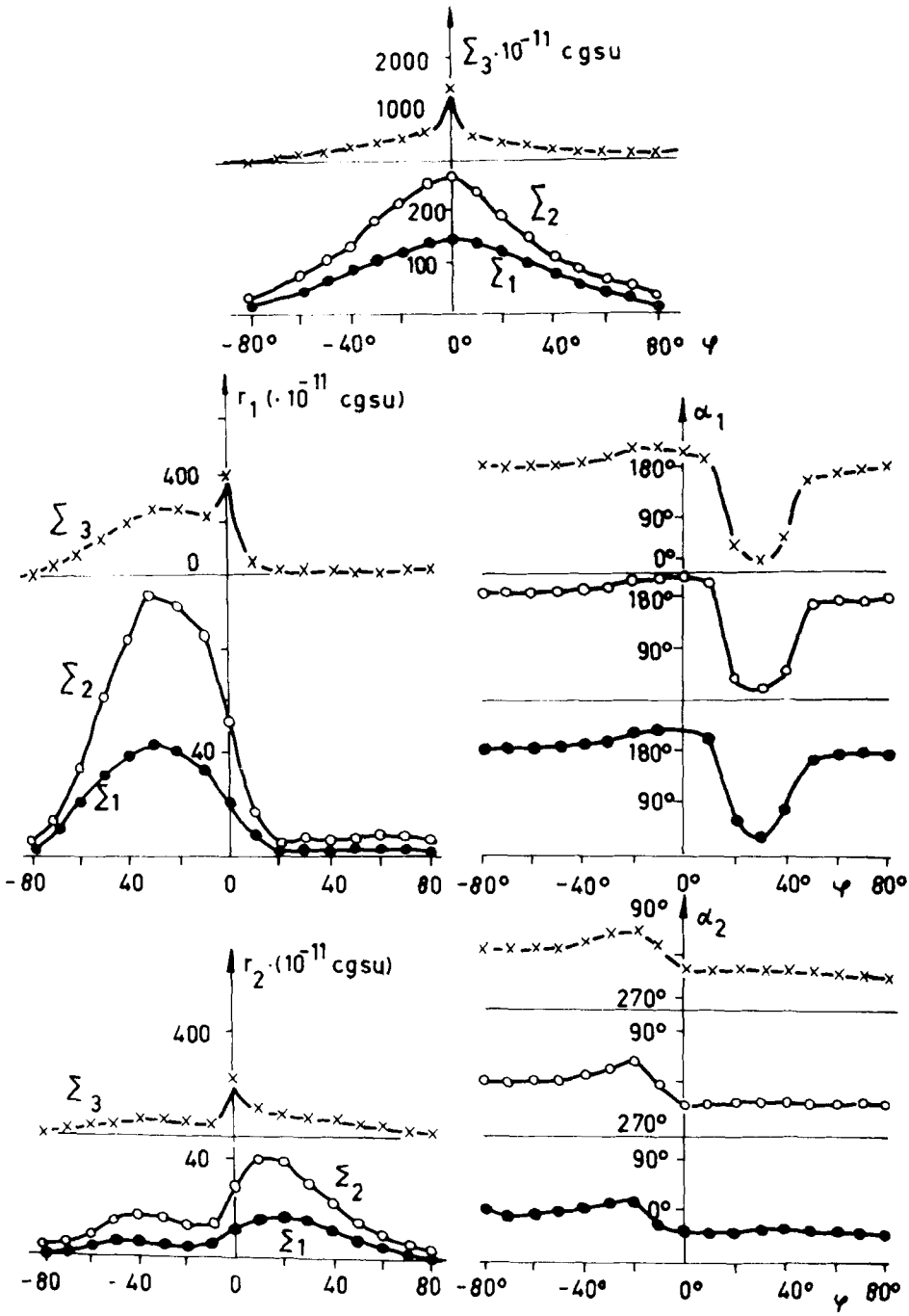

Fig. 10. Daily mean values, amplitudes r_i and phases α_i of the first two harmonics of the UT-variation of the integrated conductivities Σ_1, Σ_2, Σ_3.

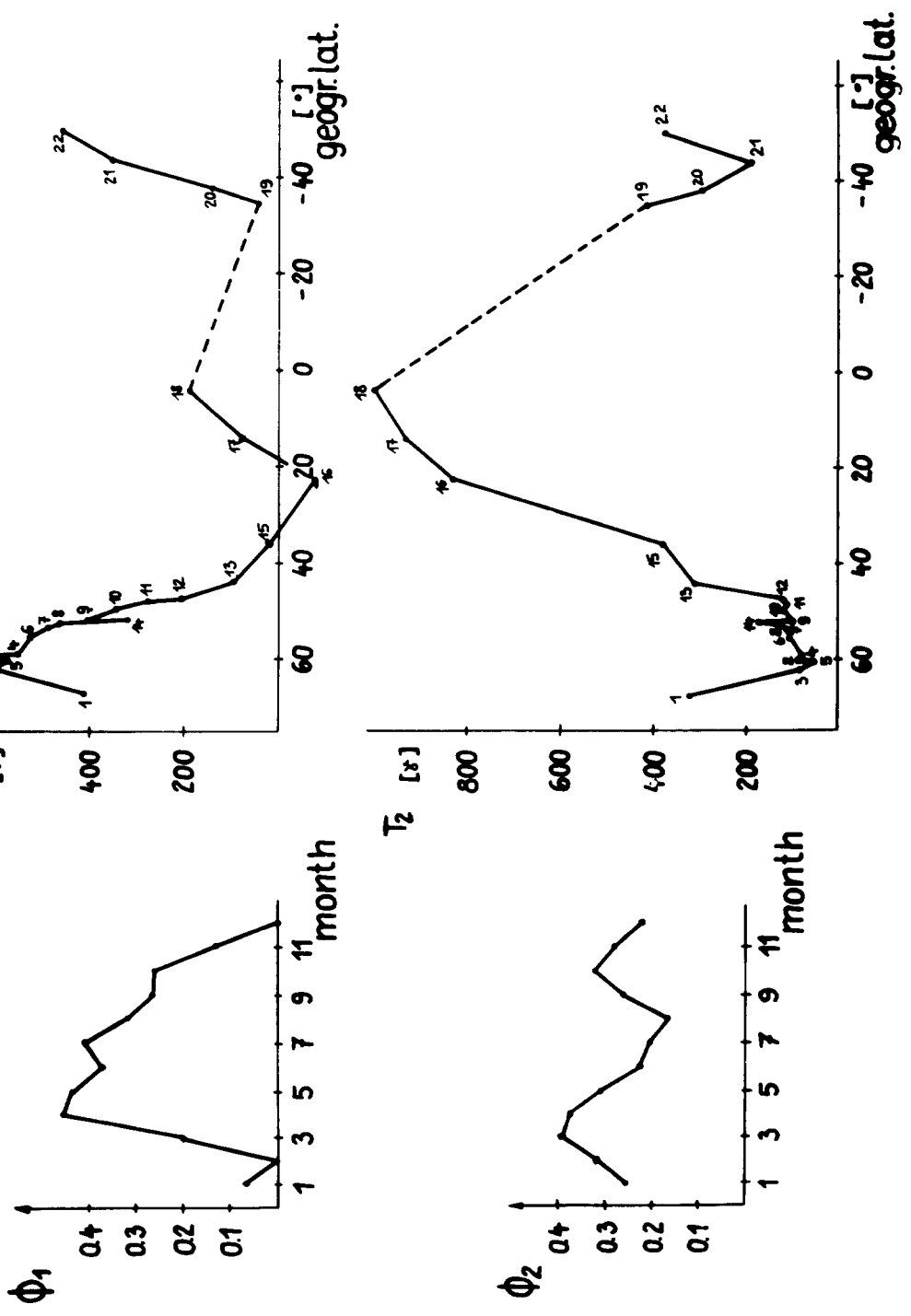

Fig. 11. Annual (upper part) and semi-annual (lower part) variation of the summed ranges of the H-component and their dependence on latitude, presented in non-orthogonal natural functions by Vertlib, Wagner (1977). (Numbers in the latitudinal curve represent different observatories.)

years 1952 to 1961. Median monthly Sq-variations have been calculated for each observatory. In these calculations averaged night-time data have been used as reference level. To amplify the effect of the seasonal variations summed ranges (the sum of the absolute values of the 24 mean hourly values) have been used. The method of principal components (Vertlib and Wagner, 1970, 1977) has been used to derive the seasonal and latitudinal dependencies from the complete data set for all 22 observatories. This method leads to a description of the seasonal (τ = number of the month) and latitudinal (φ) dependencies by

$$F(\tau, \varphi) = \sum_{k=1}^{1} \phi_k(\tau) T_k(\varphi), \qquad 1 \leq \tau_{\max} . \tag{2.10}$$

For the H-component an annual variation as well as a 'semi-annual' variation of the summed ranges has been found (Figure 11). The upper part of Figure 11 shows the annual variation and its dependence on latitude whereas the lower part shows the 'semi-annual' variation and its latitudinal dependence. Both variations show a symmetric behaviour to the equator. In this connection it must be mentioned that the data from the southern hemisphere have been combined with the data from the northern hemisphere in that manner that the summers coincide. The amplitude of the annual variation decreases with decreasing latitude in accordance with the higher variation of the energy input time in dependence on season in higher latitudes. The 'semi-annual' variation shows two maxima around the equinoces. The maximum in spring is higher than in autumn. The main feature of the latitudinal dependence of the 'semi-annual' variation consists in a strong increase of the amplitude of this variation from about 45° geographic latitude towards the equator and only small variations towards higher latitudes.

In contrast to these properties of the H-component, for the D-component only an annual variation has been found. The amplitude of this annual variation decreases with decreasing latitude. In the D-component no pronounced 'semi-annual' variation seems to exist. Speaking in terms of equivalent current systems these results seem to indicate that the 'semi-annual' variation of the amplitude of the Sq-variations characterized by the summed ranges has to be explained by 'semi-annual' variations of the strength of a nearly azimuthal current. Independently, Schäfer (1978) found additional hints to believe that there exists such a zonal current.

An increase in solar activity (i.e. of the R-number) in both components (H, D) creates only an increase in the amplitude but no principal changes in the seasonal and latitudinal dependencies. (Vertlib and Wagner, 1977).

Another group of authors investigated the seasonal variations of the mean Sq-field, using the spherical harmonic analysis i.e. analysing the seasonal variation of the total currents of both vortices and of the positions of the foci. For illustration, Figure 12 shows the results of Mishin *et al.* (1966) for the IGY (American sector). They found an annual and a 'semi-annual' variation, which for the high solar activity conditions of the IGY may reach the same amplitude as the annual. The seasonal variations reach a maximum amplitude of 30% of the mean annual value. A more

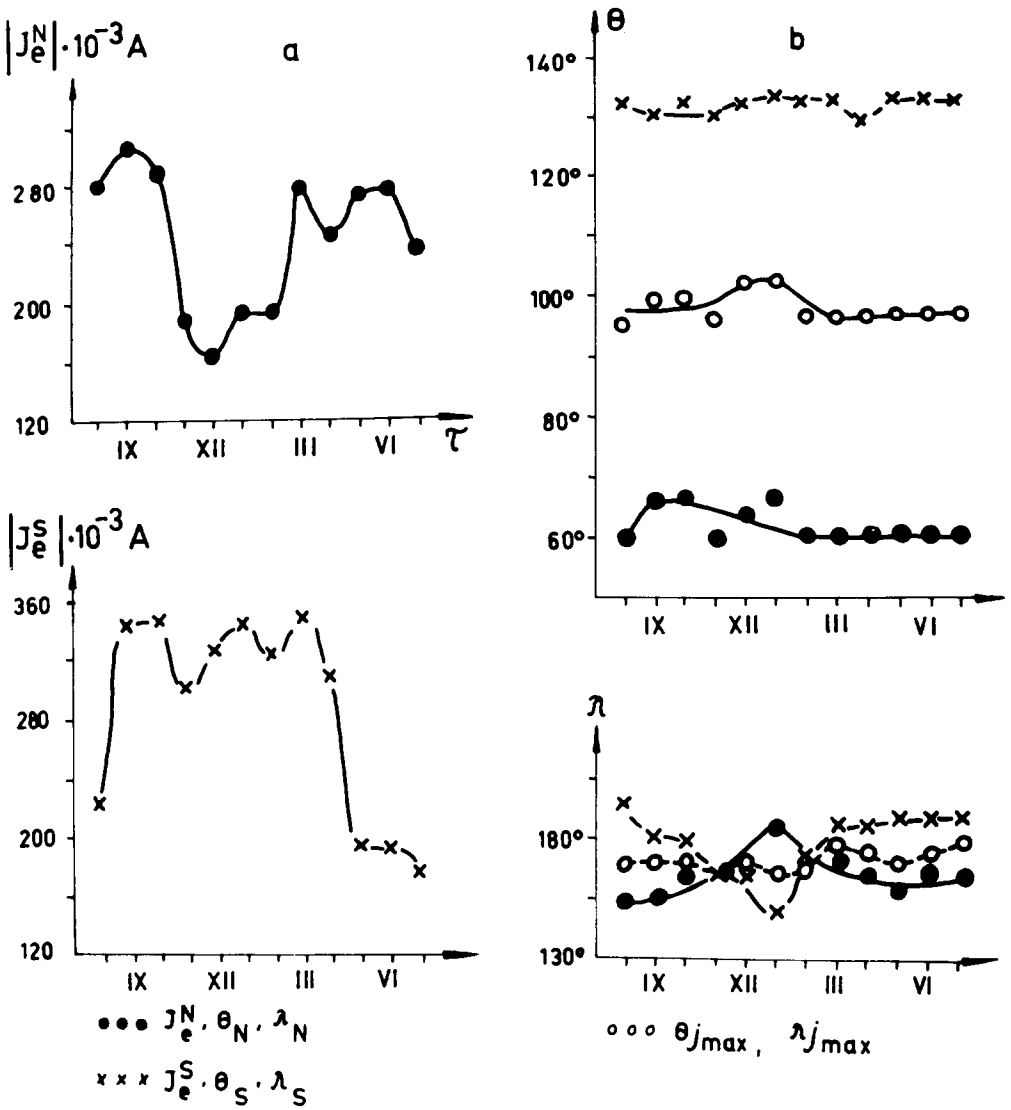

Fig. 12. Seasonal variation of the total current (a) and the positions of the foci (b) of the *Sq*- vortices in the American sector, IGY-data after Mishin *et al.* (1966).

detailed investigation shows that the ratio annual variation/mean annual value for the northern hemisphere is 0.20, for the southern 0.26, but the ratio of the annual variation on both hemispheres $(\Delta J_S)^a/(\Delta J_N)^a$ is 1.6 due to the fact that the mean annual value on the southern hemisphere is somewhat higher. The maximum of the annual variation occurs at local summer, that of the 'semi-annual' variations at the equinoces. The focus latitudes show only a very small but complicated variation. For the longitude (local time) of the focus they found a wave-like variation of considerable amplitudes which is greater for the southern, smaller for the northern focus. For

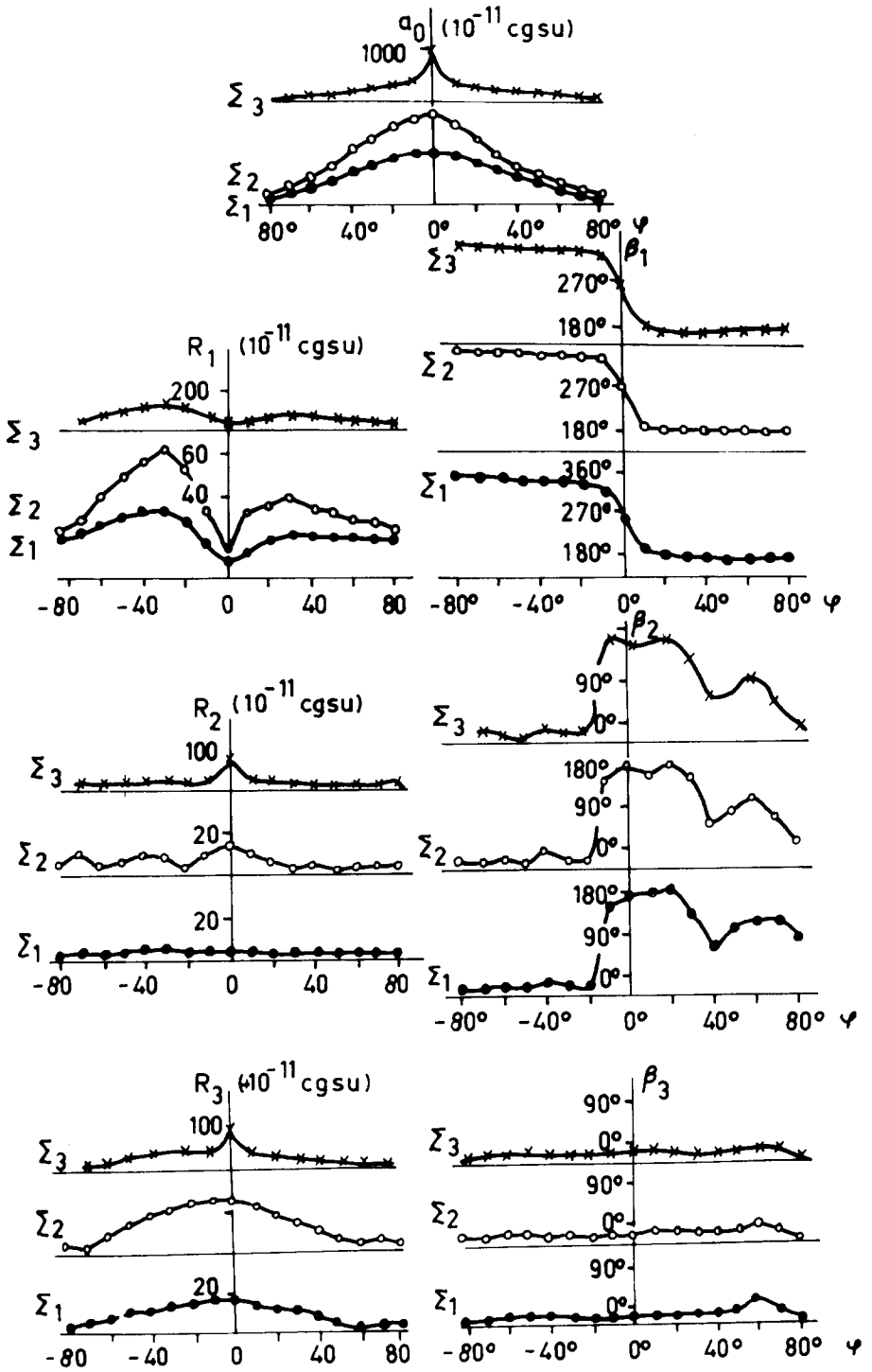

Fig. 13. Annual mean value, amplitudes R_i and phases β_i of the first three harmonics of the seasonal variation of the integrated conductivities Σ_1, Σ_2, Σ_3.

northern summer and the equinox the northern focus has a lower longitude, i.e. occurs earlier, than the southern one. That means that during these months the northern vortex is shifted towards the morning hours in comparison with the southern vortex.

2.2.4. *Seasonal Variation of the Conductivity*

Seasonal and especially annual variations are assumed to be an effect of the declination of the Earth' rotation axis towards the ecliptic plane i.e. the antisymmetric inflow of solar energy. Therefore, it must be checked how this fact is reproduced in the electric conductivity. These calculations have been done for noon-values by Nemtzova and Mishin (1970) for different latitudes in the same manner as described above. The variations are rather complicated, showing at least

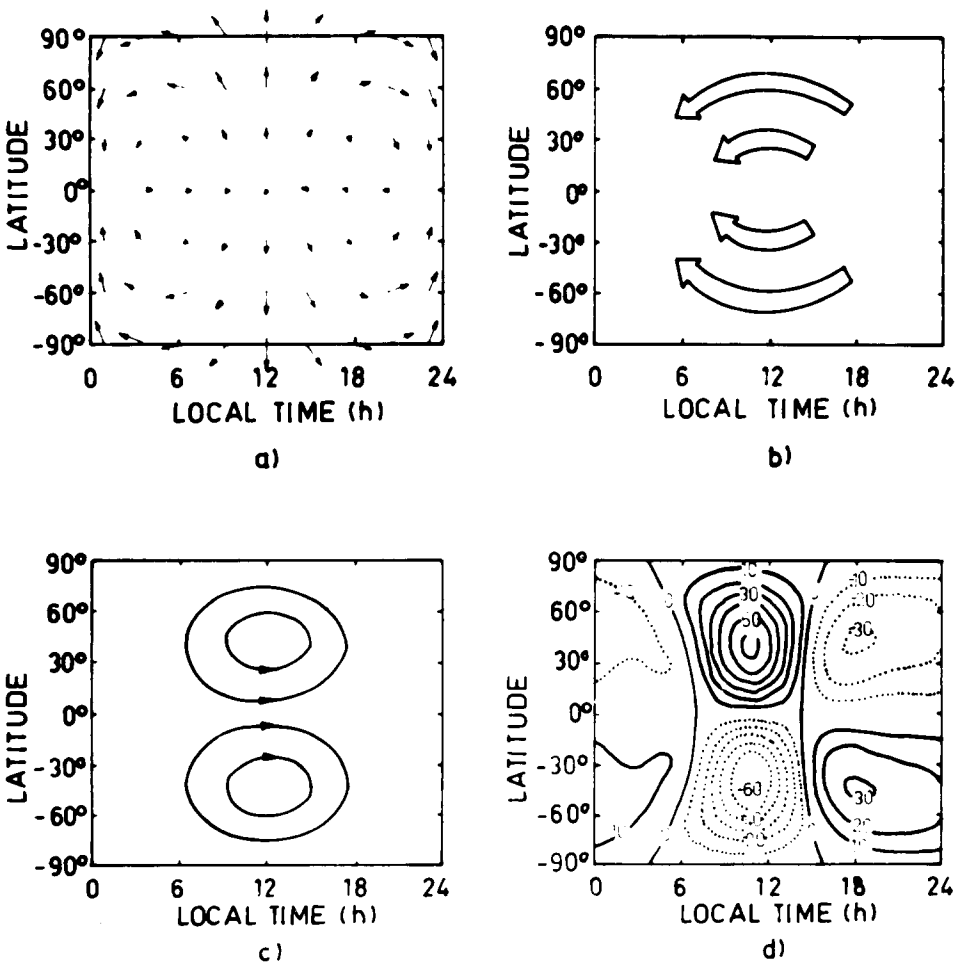

Fig. 14. Two-dimensional scheme of the generation of the *Sq*-current system. (a) (1, −2) tidal wind field. (b) resulting electromotive forces. (c) horizontal current system. (d) equivalent current system after Chapman and Bartels (1940).

'semi-annual' variations besides the annual one. For the integral conductivities at local noon these data have been described by

$$\Sigma_k = \sum_{m=0}^{3} R_{k,m} \cos(m\tau - \beta_{k,m}), \qquad k = 1, 2, 3, \tag{2.11}$$

when τ is the number of the month. The results are shown in Figure 13. The maximal amplitudes of the annual variation are greater at the southern hemisphere, the phases are independent on latitude and maxima occur at local summer. Since the other components are smaller and rather complicated, they will not be described in detail. A comparison with the corresponding data for the *Sq*-field (see Figure 12) shows that the annual variations have the same phases and approximately the same ratio of annual variation to the annual mean value. The relative amplitude of the 'semi-annual' variation in *Sq* is considerably higher than for the conductivity. In this case also the phases are different. Therefore, it seems to be impossible to explain the 'semi-annual' variation without taking into account other processes independent on the conductivity (see Wagner, 1968; Mishin, 1976). The next step, now, is to check whether the annual variation of the conductivity is able to produce the observed variations of the *Sq*-field.

2.2.5. *Summary of the Most Important Facts and Construction of an Empirical Three-Dimensional Model for the Sq-Currents*

The characteristics of the *Sq*-fields and their sources, which have been described above may be summarized in the following way:

(I) The *mean annual system* of equivalent *Sq*-currents consists of two vortices.

(a) The direction of the equivalent currents is anticlockwise in the northern hemisphere and clockwise in the southern hemisphere.

(b) The density of the currents is 2 to 5×10^1 A km^{-1} in middle latitudes and $1\text{–}2 \times 10^2$ A km^{-1} near the geomagnetic equator.

(c) The foci are situated in a latitude of about $\varphi_f = 30\text{–}40°$.

(d) The focus in the southern hemisphere has been found for $t_f > 12:00$ LT and in the northern hemisphere for $t_f < 12:00$ LT. The time difference between both hemispheres is $\Delta t_f \approx 1$ hr.

(e) The boundary between the two vortices follows the geomagnetic equator.

(II) *Seasonal variations* lead to a modulation of the intensity of the (daily averaged) *Sq* vortices (I_N, I_S) and of the coordinates of the foci t_f, φ_f. The variations of I_N, I_S show an annual and a semi-annual period. A maximum of the annual variation occurs in local summer, the maxima of the semi-annual variation during the equinoxes.

(a) The amplitudes of both waves seem to be linear correlated and show a ratio $r_2/r_1 = 0.6$.

(b) The ratio $I_{\text{summer}}/I_{\text{winter}} = 1.5$ is smaller than it has to be expected from the two-dimensional dynamo theory.

(c) The time difference of the foci in both hemispheres Δt_f varies from about 2.5 hr during northern summer to about 0 during northern winter and is close to 1.0 hr during the equinoces.

(d) The maximum of the semi-annual variation during northern spring is higher than during autumn. The main feature of the latitudinal dependence of the semi-annual variation of the H-component consists in a strong increase of the amplitude from about 45° geographic latitude towards the equator and only small variation towards higher latitudes. There is no pronounced semi-annual variation in the D-component.

(e) An increase in solar activity creates only an increase in the amplitude but no principle changes in the seasonal and latitudinal dependencies.

(III) *UT-variations* lead also to a modulation of the intensities I_N, I_S, and of the coordinates of both foci.

(a) The variations of the intensity I on the northern and southern hemisphere are nearly in phase.

(b) The amplitude of this modulation reaches about 40% of the mean value; the amplitude is considerable higher in the southern hemisphere in comparison with the northern one.

(c) The time of the occurrence of the maxima of the modulation shows a seasonal variation but is found to be always in the interval 12:00–18:00 UT.

(d) The focus of the S_q vortex shows an anticlockwise rotation in the northern and a clockwise one in the southern hemisphere.

(e) The time difference of the occurrence of the foci in both hemispheres Δt_f shows a sinus variation with UT with an amplitude $\geqslant 2.00$ hr and a maximum close to 12:00 UT.

(f) During the equinoces one finds for any moment UT $\Delta t_f > 0$.

Let us now try to understand these dependencies in a qualitative way using the theory of the atmospheric dynamo:

The tidal wind mode (1, −2) has been drawn in Figure 14a, the corresponding dynamo field $\mathbf{v} \times \mathbf{B}$ in Figure 14b assuming a central dipole field for $\mathbf{B}$. Approximatively the dynamo currents in the two-dimensional theory may be described by $\mathbf{j} = \Sigma_3(\mathbf{E} + \mathbf{v} \times \mathbf{B})$. These dynamo currents are shown in Figure 14c. Obviously these currents show all characteristics mentioned for the mean annual Sq-field in (I) except (I.d). If one, however, takes into consideration that in the real geomagnetic (nondipolar) field the daily averaged angle between the magnetic and the noon-time geographic meridian is approximately equal to Δt_f, also the characteristic (I.d) is at least qualitatively understandable.

The question arises whether the model described in Figure 14c, i.e. the two-dimensional dynamo model is also suitable for the description of the characteristics of seasonal and UT-variations of the Sq-system (see points (II) and (III)). Using the two-dimensional dynamo theory Nagata and Sugiura (1948), Akopyan (1966), Afraimovitch *et al.* (1966), Zaitzev (1968) calculated the UT variations I_N and I_S and found that they show an antiphase behaviour with extrema at 16:50 and 04:50 UT,

i.e. during noon and midnight on the northern geomagnetic hemisphere. The reason for this antiphase behaviour must be seen in the precession of the magnetic axis: Let us assume that the generation region for the Sq-currents is fixed in a solar coordinate system so that only the dynamo field $\mathbf{v} \times \mathbf{B}$ produces an UT-variation proportional to the UT periodic changes of the magnetic dipole field. The precession of the dipole axis leads for the same moment to the maximal value of the magnetic field in the northern vortex and the minimal value in the southern vortex region and vice-versa. Therefore, it is clear that from the two-dimensional theory one will find an antiphase behaviour of the total current in both hemispheres.

In the papers mentioned above the geomagnetic main field has been approximated by a dipole and the electrical conductivity by scalar laws. Mishin *et al.* (1970, 1971, 1976) calculated UT-variations using two-dimensional dynamo theory with more realistic magnetic fields and electric conductivities, but in principle they found the same result i.e. an antiphase UT-variation of the currents. The same authors also tried to explain the seasonal variation of the Sq-currents using the two-dimensional theory. The main result from these calculations was that the ratio $I_{\text{summer}}/I_{\text{winter}}$ reaches values which are much higher than 1.5. In any case using the two-dimensional theory results in an increase of the north-south asymmetry of the intensity of the dynamo currents in comparison with the experimental data. To solve this disagreement and to explain the UT and seasonal characteristics of the Sq-field (see (II.b) and (III.a)) it is necessary to include the electric coupling between the two hemispheres and field-aligned currents into the model. An analogous conclusion has been drawn by Van Sabben and Yanagihara (1971) from an analysis of the annual variation of Δt_f (see (III.c)).

The resulting model of the field-aligned currents has been shown in Figure 15a. The currents are flowing into the summer hemisphere within the inner part of the Sq-vortex and are flowing out of this hemisphere at the periphery in order to avoid the creation of an antisymmetric polarization field. In the summer hemisphere the field-aligned currents create Hall currents flowing clockwise and in the winter hemisphere Hall currents flowing anticlockwise. In this manner the field-aligned currents result in a decrease of the summer Sq-vortex and an increase of the intensity of the winter Sq-vortex i.e. decreasing the north-south asymmetry in correspondence with what is needed in order to explain the measurements. If one assumes that the main magnetic effect on the Earth's surface comes from the central part of the system of field-aligned currents, the model given in Figure 15a is able to explain the observed annual variation of Δt_f (see (III.c)). The estimations (Mishin *et al.*, 1970, 1971, 1976; Yanagihara, 1971) show that the average density of the field-aligned currents is 10^{-12} A cm^{-2} and near the foci $\approx 10^{-11}$ A cm^{-2}.

Let us now discuss Figure 15b, which should help us to understand qualitatively the physics of the observed phenomena. Let us assume that on one of the hemispheres e.g. the southern one a Sq similar electric field E_S (clockwise field) is generated. Due to the anisotropy of the electric conductivity this field results in a vortex of Pedersen-currents ($\Sigma_{1S} \cdot E_S$) and Hall-currents ($\Sigma_{2S} \cdot E_S$) directed away

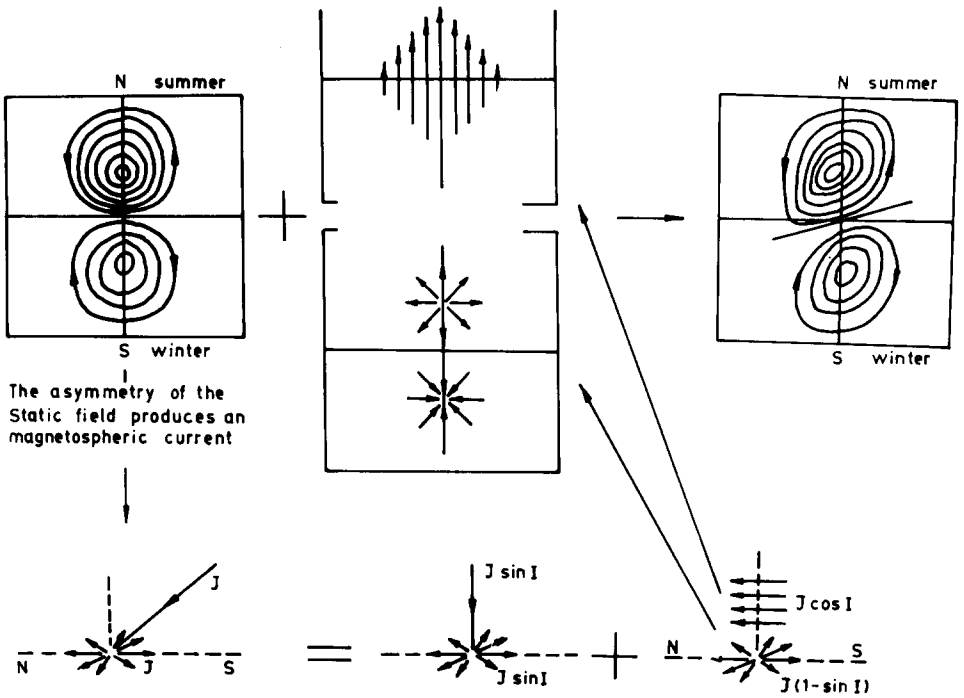

Fig. 15. Threedimensional current systems derived by Yanagihara (1971) for northern summer and Mishin (1976) for northern summer (a) and northern winter (b).

from the point P, where P is the centre of the vortex (see Figure 15b). The existence of these Hall-currents means that there flows a field-aligned current $k \cdot \Sigma_{1N} \cdot E_p$ from the conjugated point P' in the northern hemisphere into the southern hemisphere. The polarization field E_p can easily be calculated from the condition that the current flowing from the northern hemisphere from point $P'(\Sigma_{1N} \cdot E_p)$ is equal to that current which flows at P into the southern hemisphere $(\Sigma_{2S} \cdot E_S - \Sigma_{1S} \cdot E_p)$; this leads to the relationship $E_p = (\Sigma_{2S}/(\Sigma_{1N}+\Sigma_{1S})) \cdot E_S$. Further $k = \pi R_0$ where R_0 is the radius of the vortex. The polarization field E_p creates a current vortex in the northern hemisphere, which is magnetically conjugated to the southern one. It can be shown that the current in the northern vortex flows anticlockwise i.e. the resulting current in the northern hemisphere is also Sq-like as that in the southern hemisphere. This fact is a key-point for the understanding of the main tendencies of the UT-variations of I_N, I_S, which has been mentioned in (III.a) and of the relatively low ratio I_{summer}/I_{winter} (see (II.b)). Summarizing the ideas described above it is possible to formulate equations for the current intensity in the vortices in both hemispheres as

$$I_N = [\Sigma_{1N} + \Sigma_{2N}^2/(\Sigma_{1N}+\Sigma_{1S})] \cdot E_N + [(\Sigma_{2N} \cdot \Sigma_{2S})/(\Sigma_{1N}+\Sigma_{1S})] \cdot E_S$$

$$I_S = [\Sigma_{1S} + \Sigma_{2S}^2/(\Sigma_{1N}+\Sigma_{1S})] \cdot E_S + [(\Sigma_{2N} \cdot \Sigma_{2S})/(\Sigma_{1N}+\Sigma_{1S})] \cdot E_N \quad (2.11)$$

Mishin (1976). Using once more the condition that the field-aligned current $j_\parallel$ is

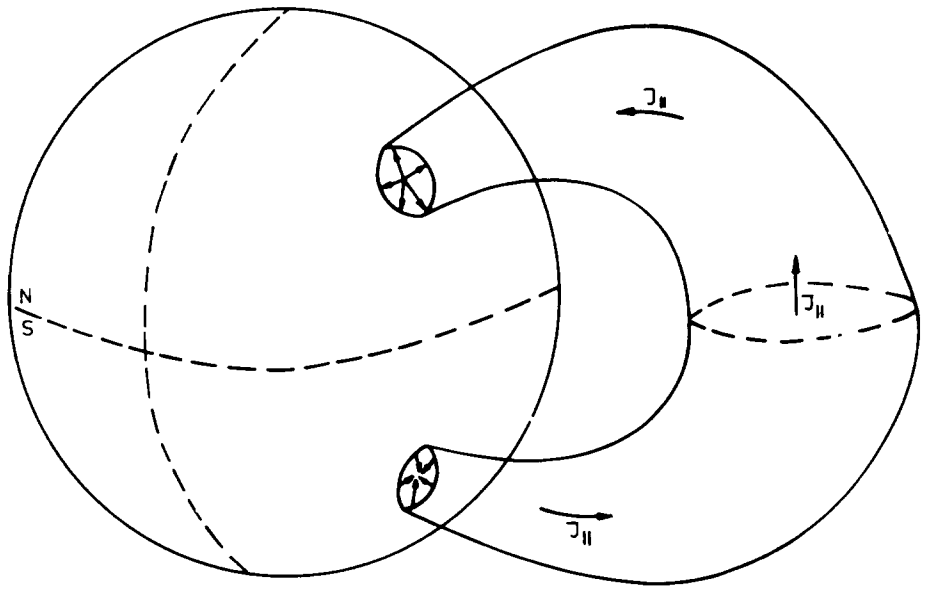

Fig. 15a.

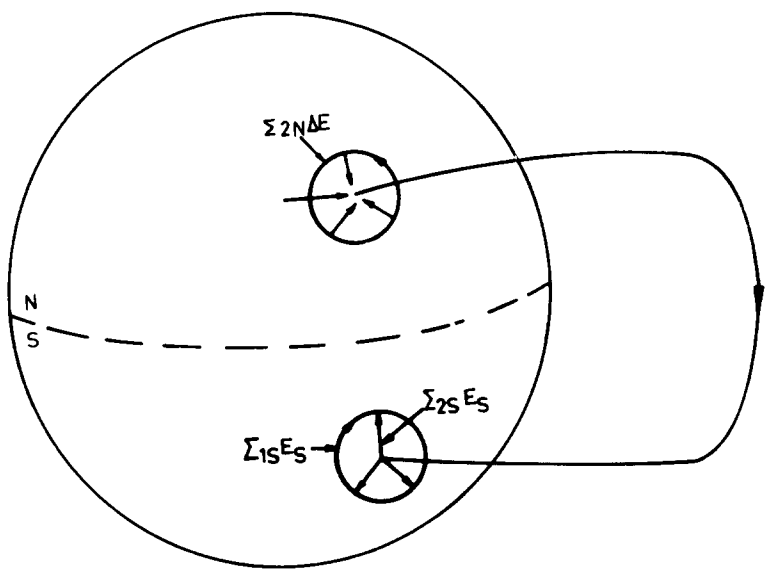

Fig. 15b.

equal to the inflowing current, i.e. $\pi \cdot R_0^2 \cdot j_\parallel = 2\pi \cdot R_0 \cdot \Sigma_1 \cdot E_p$, one finds

$$j_\parallel = 2(\Sigma_{1N} \cdot \Sigma_{2S} \cdot E_S - \Sigma_{1S} \cdot \Sigma_{2N} \cdot E_N)/(\Sigma_{1N} + \Sigma_{1S})\,/R_0 \tag{2.12}$$

with R_0 for the radius of the vortex and assuming the direction towards the southern hemisphere as the positive field-aligned current direction.

These simple equations give the possibility to estimate the general influence of the coupling between both hemispheres and to check, whether the introduction of such a quasi-short-circuit coupling would result in a better agreement between the observations and the models. This estimation will be performed as well for the UT-variations as for the seasonal variations.

(a) UT-variations of the intensity of the dynamo-currents resulting from the three-dimensional model (2.11): Let us, as generally, assume that the UT-variation of the electric field is due to the diurnal shift of the S_q-vortices relatively to the wind fields. Then the phases of the UT-variation of the electrostatic field on both hemispheres will differ by 180°. Using the abbreviations

$$\begin{aligned} &\Sigma_N = \Sigma_{N0}[1 + \varkappa r \cos(T - \alpha)], \quad \Sigma_S = \Sigma_{S0}[1 + r\cos(T - \beta)]. \\ &E_N = E_{N0}[1 + \rho \cos(T + \gamma_N)], \quad E_S = E_{S0}[1 + \rho \cos(T + \gamma_S)], \\ &\Sigma_{20}/\Sigma_{10} = \mu, \quad \Sigma_{S0}/\Sigma_{N0} = K, \quad E_{S0}/E_{N0} = K' \end{aligned} \tag{2.13}$$

this means $\gamma_N = \gamma = 70°$, $\gamma_S = \gamma + 180°$. As has been described in (2.2.2) and is demonstrated in Figure 10, the electric conductivity also shows a UT-variation differing between the northern and southern hemisphere. If one assumes that the conductivity conditions are mainly determined by the conductivity in the central region of the S_q-vortices from Figures 10 and 13, one finds

$$\begin{aligned} &\alpha = \beta = 200°; \qquad \mu = \sqrt{2}; \qquad K_{XI\text{–}II} = 2; \\ &K_{V\text{–}VIII} = 0.5; \qquad \varkappa = 0.0 - 0.2 \end{aligned} \tag{2.14}$$

with $K = K'$,

$$\begin{aligned} &\Delta i = 0.5[i_{XI\text{–}II} - i_{V\text{–}VIII}], \qquad \Sigma i = [i_{XI\text{–}II} + i_{V\text{–}VIII}], \\ &(i')_{XI\text{–}II} = \Sigma i + \Delta i, \qquad (i')_{V\text{–}VIII} = \Sigma i - \Delta i, \end{aligned} \tag{2.15}$$

and

$$\begin{aligned} &i' = [[1 + K_1 r \cos(T - 200°) + K_2 \rho \cos(T - 70°)] \\ &L = \Sigma_0 E_0 \end{aligned} \tag{2.16}$$

from (2.11), (2.13), (2.14), and (2.15) it is possible to determine the coefficients L, K_1, K_2 in (2.16).

Averaging the values of the amplitude for the first harmonic of the UT-variation of Σ_2 for medium latitudes of the southern hemisphere from Figure 10 we find $r = 0.3$. The amplitude of the UT-variation of the electric field ρ can be estimated only very roughly. Data from Maeda (1957) show that ρ is of the order of 0.1. We used a value of $\rho = 0.15$. With these estimated rough values it is possible to calculate the UT-dependence of the currents $i_N(T)$ and $i_S(T)$ and the seasonal variations of these UT-dependent currents $\Delta i = (i)_{XI\text{–}II} - (i)_{V\text{–}VIII}$. The results of these rough estimations have been drawn in Figure 16. The points respectively crosses give the

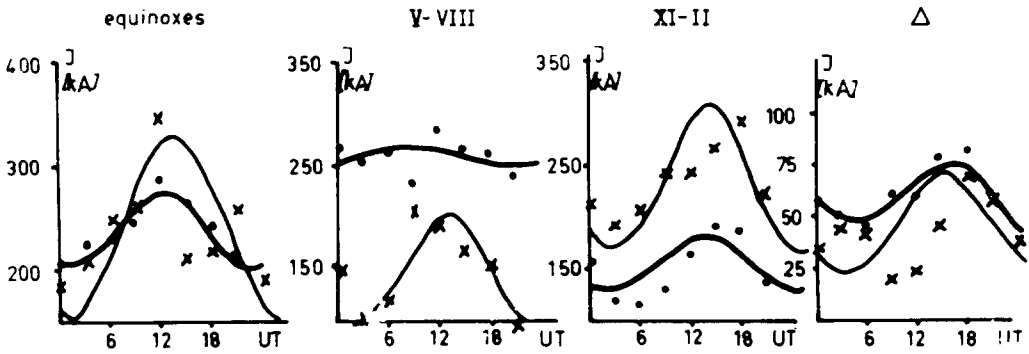

Fig. 16. Comparison of the observed general trend for the UT-variation of the total currents in the northern and southern vortices for different seasons with rough theoretical threedimensional estimations (dots (N) and crosses (S)).

results of the estimations, whereas the curves show the trend of the principal observed data (drawn more in detail in Figure 7). In spite of some differences, the general agreement between the estimations and the measurements is quite satisfactory.

(b) UT-variations of the focus shift Δt_f between both hemispheres estimated from (2.12): Whereas (2.11) gave us the possibility for a comparison with current density, the Equation (2.12) allows to estimate the field-aligned currents resulting from the coupling of both hemispheres. One result of the introduction of such field-aligned currents is a shift between both foci (see Figure 15a and Yanagihara, 1971). Assuming that the foci of the S_q-vortices represent geomagnetically conjugated points on the geomagnetic noon meridian in latitudes of 30–40°, for the UT-variation of Δt_f one would expect a simple oscillation with the following characteristic: The maximum should occur at 10:30 UT and the amplitude of the diurnal variation should be $2 \times 23° \approx 3$ hr. The observed values Δt_f, however, have their maximum not in the neighbourhood of 10:30 UT but near 12:00 UT, and the diurnal variation of the coordinates of the foci is not a monotonical one. The amplitude of this variation is considerable higher in the southern hemisphere than in the northern one (see Figure 7). All these facts lead to the assumption that in addition to the trivial part of the UT-variation described above there exists a second contribution to the UT-variation with an amplitude of 1–2 hr and a maximum in the interval of 12:00–18:00 UT. This second contribution may be a result of the field-aligned currents described by (2.12). Taking into consideration, only the first harmonics of the electro-conductivity (see Figure 10) and assuming

$$\Sigma_{1N} + \Sigma_{1S} \approx (0.5\Sigma_0)[1 - 0.5r \cos(T - \alpha)]^{-1}$$

one finds from (2.12)

$$j_\parallel \approx (4/R_0)\, \mu\, \Sigma_0 (E_S - E_N)\,. \tag{2.17}$$

For the near noon region, one finds a field-aligned current $j_\parallel$ which is directed into the

northern hemisphere and has its maximum near 13:00 UT. For $|E_S - E_N| \approx 1\ \text{mV m}^{-1}$, $R_0 = 2000$ km, the estimations lead to $j_\parallel \approx 10^{-12}\ \text{A cm}^{-2}$. According to Yanagihara (1971) such field-aligned current leads to a shift of the foci of $\Delta t_f \approx 1$ hr, which corresponds to the expected value for the second contribution.

(c) Influence of the coupling between both hemispheres on the annual variation of i_N, i_S estimated from (2.11): As has been discussed above, two-dimensional dynamo theories result in an overestimation of the annual variation. Since the first terms in the right-hand side of Equation (2.11) for i_N, i_S resp. more or less coincide with the formula $\mathbf{j} = \Sigma_3 \mathbf{E}$ describing approximatively the current density in two-dimensional models, the second part of the Equation (2.11) gives an estimation of the influence of the field-aligned current on current densities. Discussing the annual variation of the current density these second terms on the right-hand side of (2.11) are of great importance. These terms are due to the antisymmetry of the electro-conductivity and the winds on both hemispheres creating current densities approximatively described by the first terms, and lead to a decrease of the annual variation of i_N, i_S. If the ratio $i_{\text{summer}}/i_{\text{winter}}$ is about 4 for the two-dimensional dynamo-models (Mishin, 1976), from (2.11) one finds only a ratio of about 2, which is close to the observed values.

(d) Estimation of the annual variation of the focus shift Δt_f resulting from (2.12): Assuming for simplicity $\Sigma_2 = 2\Sigma_1$, $\Sigma_{\text{summer}} = 2\Sigma_{\text{winter}}$, one finds from (2.12)

$$j_\parallel = \frac{8}{3R_0} \Sigma_{1\ \text{winter}} \quad (E_N - E_S).$$

If $E_{\text{summer}} > E_{\text{winter}}$, the field-aligned current $j_\parallel$ flows into the summer hemisphere and leads consequently to positive values Δt_f during northern summer and to negative values during northern winter. The density of the field-aligned currents is $j_\parallel \approx 10^{-12}\ \text{A cm}^{-2}$ leading to an amplitude of the annual variation of 1–2 hr. The amplitude and the phase of this annual variation coincides qualitatively with the observations.

(e) Influence of the coupling on the semi-annual variation: It cannot be decided today, whether it would be possible to explain the observations about the semi-annual variation in the same manner. However, since in (2.11) and (2.12) there occur products of the type $\Sigma_N \cdot \Sigma_S$, both showing an annual variation, one has to expect also a semi-annual component in the field-aligned currents. It may be that within a self-consistent calculation of $j_\parallel$ and $\mathbf{E}$ not only the field-aligned current, but also the total electric field and therefore, also the current i_N, i_S will show an oscillation with maxima around the equinox.

These estimations and discussions based on a very simple three-dimensional dynamo model indicate that it should be possible to explain the physical mechanisms leading to nearly all observations summarized at the beginning of this paragraph by three-dimensional dynamo models. The most important simplifications within this model consist in neglecting the spatial variation of the ionospheric electro-conductivity and in replacing the equivalent ionospheric currents by one-dimensional

current vortices. For the authors, it was surprising and encouraging that such a simple superposition of the influence of field-aligned currents gave the possibility to explain a great number of observations, which could not be explained on the base of two-dimensional models.

In this review paper, we described only regular variations. It should rather be mentioned that there exists a whole complex of irregular variations of the electric field and the current systems in the undisturbed plasmasphere, which are correlated with variations of the velocity, the density and the magnetic field of the solar wind. The amplitudes of these irregularities may reach the same order of magnitude as the regular variations. Since this topic is out of the scope of this review, we only should like to refer the review papers by Kane (1976), Mishin (1976, 1977, 1978, 1979).

Whereas this section results in an empirical model which gives us the possibility to reach a qualitative understanding of some of the new facts which have been found during recent years in the following section we will describe the quantitative theory of two-dimensional and three-dimensional dynamo models and summarize to what extent it has been possible to check the qualitative ideas quantitatively.

3. Large-Scale Dynamo-Electric Fields and Currents

Large-scale dynamo-electric fields and currents are connected with two different phenomena in the Earth's ionosphere and plasmasphere.

– Horizontally closed current systems are driven by N–S symmetric dynamo-action. These horizontal currents are flowing in a relatively thin current layer. Therefore, they can be assumed to be (approximatively) 'two-dimensional'. The electrostatic field connected with these currents is the dominating ionospheric symmetric electric field at median latitudes and directed perpendicular to the magnetic field. The relevant physical process will be discussed in Section 3.1.

– Global 'three-dimensional' currents are driven by asymmetric dynamo-action. These currents are closed through plasmaspheric field-aligned currents. They are driven by antisymmetric electric fields. Their component perpendicular to the magnetic field can be neglected in comparison with the symmetric electric field. Models for 'three-dimensional' current systems will be described in Section 3.2.

3.1. Symmetric Dynamo-Electric Fields

The physical processes resulting in dynamo-electric fields have been discussed in Section 1. The relevant potential equation can be found to be

$$\operatorname{div} \boldsymbol{\sigma} \operatorname{grad} S = \operatorname{div} \boldsymbol{\sigma}(\mathbf{v}_n \times \mathbf{B}_0) , \tag{1.2}$$

where $\mathbf{B}_0$ represents the geomagnetic main field, and $\boldsymbol{\sigma}$ has been computed with respect to this $\mathbf{B}_0$. This linearizing procedure is possible due to the relative smallness of the resulting variations $\delta \mathbf{B}$ of the magnetic field with respect to $\mathbf{B}_0$. Furthermore, it can be shown that the large-scale charge accumulations $q = -\varepsilon_0 \Delta S$, connected with

(1.2) are neglectably small compared with the ionospheric electron density. Therefore, $\boldsymbol{\sigma}$ does not depend on S and the potential S can be computed from (1.2) using models of the 'parameter fields' $\boldsymbol{\sigma}$, $\mathbf{v}_n$ and $\mathbf{B}_0$.

As has been discussed in Section 1 the following three 'physical pictures', which result from the ionospheric distribution of the electro-conductivities σ_0, σ_1, and σ_2 (see Figure 1), can be used to simplify the procedure of solution of (1.2). At least, these 'pictures' are obvious properties of the solutions of (1.2) for real ionospheric conditions. They are:

– Due to the dominance of σ_0 with respect to σ_1 and σ_2 the 'magnetic field lines' can be assumed to be electrostatic equipotentials. A weaker formulation of this is an expansion of S in powers of σ_1/σ_0 (Möhlmann, 1977).

– As will be discussed more in detail in connection with antisymmetric dynamo-effects, and as a result of $\sigma_1/\sigma_0 \ll 1$ antisymmetric electric fields are 'quasi-short-circuited'. Therefore, the dominating ionospheric large-scale dynamo-electric field is caused by 'symmetric dynamo-action' (Schäfer, 1978).

– Internally closed (short scale) radial currents do not play any essential role in the generation of (horizontally) large-scale electric fields. This follows from the approximation of a relatively thin current carrying region taking into account $(J_r/J_H) \approx (d/R) \ll 1$ with d is the thickness of the dynamo-layer and R the Earth's radius. This formula results from an order of magnitude estimation from div $\mathbf{j} = 0$.

It shall be noted here that the approximation $\mathbf{j}_r = 0$ gives the possibility to eliminate E_r from the dynamo Equation (1.2) and to derive a 'two-dimensional' equation for S, depending on latitude and longitude. Dynamo equations of this two-dimensional type have been derived first from Baker and Martyn (1953). They have been discussed extensively by Matveev in the book from Bazarzhapov *et al.* (1979). A great amount of papers in connection with the atmospheric dynamo has been based on these two-dimensional equations and referred to be within the frame of a 'two-dimensional dynamo-theory'. The simplest solution for the electric field $\mathbf{E}_0$ follows with the boundary condition mentioned above

$$0 = \mathbf{j}_r = \mathbf{e}_r \boldsymbol{\sigma}(\mathbf{E}_0 + \mathbf{v}_n \times \boldsymbol{B}_0) ,$$

where $\mathbf{e}_r$ represents the radial unit vector. Analytical solutions for S for different tidal wind fields $\mathbf{v}_n$ have been found by Möhlmann (1971, 1977). He found that these solutions for the potential S are precisely enough (in comparison of the accuracy of the available measurements of the electric field) to discuss the gross-structure of the global distribution of the ionospheric dynamo-electric fields.

This 'zero-order' solution S_0 cannot give a satisfying description of the horizontal currents. To compute them, equations of the Baker/Martyn-type (see for instance (3.12)) have to be solved (see Chapter 4 in Bazarzhapov *et al.*, 1979; Möhlmann, 1977). Equations of this type have to be solved numerically.

The most complicated way to solve (1.2) is a numerically treatment for realistic fields of $\boldsymbol{\sigma}$, $\mathbf{v}_n$ and $\mathbf{B}_0$. In this case boundary conditions have to be used to describe the influence of coupling-currents between the hemispheres.

This discussion shows that the two-dimensional theory seems to be very useful to calculate the gross-structures of dynamo-electric fields. In the following some simplifying methods for these calculations will be discussed and the results received by different authors will be critically reviewed.

3.1.1. *An Analytical Solution*

As has been shown by Möhlmann (1976, 1977) from $\mathbf{t} \cdot \text{grad}\, S_0 = 0$ and $(j_0)_r = 0$ the two ordinary differential equations ($\mathbf{t} = \mathbf{B}_0/B$) (in spherical coordinates)

$$\frac{dz}{z} = \tfrac{1}{2}(4-3z)^{1/2}\, d\varphi\,, \tag{3.1}$$

$$\frac{dS_0}{d\varphi} = -R(4-3z)^{1/2}\,\sigma_2^{-1}\,\mathbf{e}_r\,(\boldsymbol{\sigma}\mathbf{v}_n \times \mathbf{B}_0) \tag{3.2}$$

can be derived for the case of 'equipotential field lines' with $z = \sin^2\vartheta$. A centered dipole for $\mathbf{B}_0$ has been used and the dynamo-process is assumed to occur at $r = R$.

Using the wind models

$$v_r = \sum_{k=0}^{\infty} C_k \sin^k\vartheta \sin(s\varphi + \varphi_0)\,, \tag{3.3}$$

$$v_\vartheta = \cos\vartheta \sum_{k=0}^{\infty} A_k \sin^k\vartheta \sin(s\varphi + \varphi_0)\,, \tag{3.4}$$

$$v_\varphi = \sum_{k=0}^{\infty} B_k \sin^k\vartheta \cos(s\varphi + \varphi_0) \tag{3.5}$$

with s as the longitudinal wave-number the resulting zero-order potential can be shown to be of the form

$$\begin{aligned} S_0 = -M_0 R \cos(s\varphi+\varphi_0)\Bigg[& \textstyle\sum_{k=0}^{\infty} \sin^{k+1}\vartheta \left(\frac{R}{r}\right)^{(k+1)/2} \times \\ & \times \frac{\frac{k+1}{2}a^2 B_k + 2sA_k}{\left(\frac{k+1}{2}\right)^2 a^2 + s^2} + \sum_{k=0}^{\infty} \sin^{k+2}\vartheta \left(\frac{R}{r}\right)^{(k+2)/2} \times \\ & \times \frac{s\,C_k}{\left(\frac{k+2}{2}\right)^2 a^2 + s^2} + \sum_{k=0}^{\infty} \sin^{k+3}\vartheta \left(\frac{R}{r}\right)^{(k+3)/2} \frac{2sA_k}{\left(\frac{k+3}{2}\right)^2 a^2 + s^2}\Bigg] + \\ & + M_0 R \sin(s\varphi+\varphi_0)\Bigg[\sum_{k=0}^{\infty} \sin^{k+1}\vartheta \left(\frac{R}{r}\right)^{(k+1)/2} \times \\ & \times \frac{asB_k - (k+1)aA_k}{\left(\frac{k+1}{2}\right)^2 a^2 + s^2} + \sum_{k=0}^{\infty} \sin^{k+2}\vartheta \left(\frac{R}{r}\right)^{(k+2)/2} \times \end{aligned}$$

$$\times \frac{\left(\frac{k+2}{2}\right) aC_k}{\left(\frac{k+2}{2}\right)^2 a^2 + s^2} + \sum_{k=0}^{\infty} \sin^{k+3} \vartheta \left(\frac{R}{r}\right)^{(k+3)/2} \frac{(k+3) aA_k}{\left(\frac{k+3}{2}\right)^2 a^2 + s^2} \Bigg]. \tag{3.6}$$

Here the abbreviation $\sigma_1 = a\sigma_2/(1+3\cos^2\vartheta)^{1/2}$ has been used.

These equations have been used by Möhlmann in order to calculate the electrostatic potential resulting from different tidal wind modes.

3.1.2. *A Simplified Potential Equation*

As has been mentioned above the Spitzer-conductivity σ_0 at ionospheric heights is greater by orders of magnitude than the perpendicular conductivities σ_1 and σ_2. For obtaining a small dimensionless parameter $\varepsilon \ll 1$ the conductivities may be represented as follows

$$\sigma_0 = c_0 f_0(r), \qquad \sigma_1 = c_1 f_1(r), \qquad \sigma_2 = c_1 f_2(r), \tag{3.7}$$

where the dimensionless functions $f(r)$ are nearly of the same order of magnitude. Introducing now

$$\varepsilon = \frac{c_1}{c_0} \ll 1 \tag{3.8}$$

we can seek solutions of (1.2) of the form

$$S = \sum_{\nu=0}^{\infty} \varepsilon^{\nu} S_{\nu}. \tag{3.9}$$

A similar representation can be found for **E** and **j**. Consequently, the potential equation transforms now into the following hierarchy of coupled equations (Möhlmann, 1974):

$$\begin{aligned}
&\operatorname{div} f_0 \mathbf{t}(\mathbf{t} \cdot \operatorname{grad} S_0) = 0, \\
&\operatorname{div} f_0 \mathbf{t}(\mathbf{t} \cdot \operatorname{grad} S_1) = \operatorname{div} f_1 (I - \mathbf{tt})\, (\mathbf{v}_n \times \mathbf{B}_0 - \operatorname{grad} S_0) + \\
&\qquad\qquad + \operatorname{div} f_2 \mathbf{t} \times (\mathbf{v}_n \times \mathbf{B}_0 - \operatorname{grad} S_0), \\
&\operatorname{div} f_0 \mathbf{t}(\mathbf{t} \cdot \operatorname{grad} S_\nu) = -\operatorname{div} f_1 (I - \mathbf{tt}) \operatorname{grad} S_{\nu-1} + \\
&\qquad\qquad + -\operatorname{div} f_2 \mathbf{t} \times \operatorname{grad} S_{\nu-1}.
\end{aligned} \tag{3.10}$$

(I = unit tensor).

To close this hierarchy means to transform it by using physically founded assumptions into a closed finite set of coupled equations.

Such additional assumption is $j_r = 0$, meaning that vertical currents do not play any essential role in generating large-scale electrostatic fields. For the zero-order electric field this gives $\mathbf{t} \cdot \mathbf{E}_0 = 0$. The magnetic field lines can therefore be assumed to be electrostatic equipotentials. Assuming now additionally $\mathbf{t} \cdot \mathbf{E}_1 = 0$, the condition

$\mathbf{e}_r \cdot \mathbf{j}_1 = 0$ leads to a closed equation for $\mathbf{E}_0$ by using Ohm's law. This solution may be called the 'zero-order solution' for the large-scale ionospheric electric field. This has been investigated analytically for a group of atmospheric tidal wind fields by Möhlmann (1974).

The assumption $\mathbf{t} \cdot \mathbf{E}_1 = 0$, giving the basis for the zero-order solution leads to relatively simple equations. However, there is no ionospheric experimental evidence supporting this assumption (Möhlmann, 1977). Therefore a more accurate way to close the hierarchy must be investigated. From $j_r = 0$ follows

$$\mathbf{t} \cdot \mathbf{E}_1 = -\frac{\sigma_1}{\sigma_0} (\mathbf{t} \cdot \mathbf{e}_r)^{-1} \mathbf{e}_r \cdot \mathbf{E}_0 - \frac{\sigma_2}{\sigma_0} \times$$
$$\times (\mathbf{t} \cdot \mathbf{e}_r)^{-1} (\mathbf{e}_r \times \mathbf{t}) \cdot \mathbf{E}_0 + (\mathbf{t} \cdot \mathbf{e}_r \sigma_0)^{-1} \mathbf{e}_r \cdot (\boldsymbol{\sigma} \mathbf{v}_n \times \mathbf{B}_0). \tag{3.11}$$

Introducing this into the second equation of (3.10) a closed equation for S_0 can be derived. This is of the form:

$$\sigma_1 \frac{\sin \vartheta}{4 \cos^2 \vartheta} (1 + 3 \cos^2 \vartheta) \frac{\partial^2 S_0}{\partial \vartheta^2} +$$
$$+ \left[\frac{\partial}{\partial \vartheta} \sigma_1 \sin \vartheta \frac{1 + 3 \cos^2 \vartheta}{4 \cos^2 \vartheta} - \frac{\partial \sigma_2}{\partial \varphi} \frac{(1 + 3 \cos^2 \vartheta)^{1/2}}{2 \cos \vartheta} \right] \times$$
$$\times \frac{\partial S_0}{\partial \vartheta} + \frac{\sigma_1}{\sin \vartheta} \frac{\partial^2 S_0}{\partial \varphi^2} + \left[\frac{\partial \sigma_1}{\partial \varphi} \frac{1}{\sin \vartheta} + \frac{\partial}{\partial \vartheta} \sigma_2 \frac{(1 + 3 \cos^2 \vartheta)^{1/2}}{2 \cos \vartheta} \right] \frac{\partial S_0}{\partial \varphi} =$$
$$= r \operatorname{div} (I - (\mathbf{t} \cdot \mathbf{e}_r)^{-1} \mathbf{t} \mathbf{e}_r) [\boldsymbol{\sigma} (\mathbf{v}_n \times \mathbf{B}_0)]. \tag{3.12}$$

This relatively simple two-dimensional equation for the zero-order potential S_0 is of the 'Baker/Martyn-type'. The theory, the properties and the methods for solution of this type of equations in connection with the two-dimensional dynamo-theory have been discussed intensively by Matveev in the book of Bazarzhapov *et al.* (1979). For the case of constant (height-integrated) conductivities and velocity fields, derivable from a potential ψ, Matveev found solutions for the electrostatic potential and the Stoke's current function in a representation with spherical harmonics.

3.1.3. *Numerical Solution for the Electrostatic Potential*

A numerical solution of a Baker/Martyn-type equation has been derived by Dvinskikh (1974) for the electric potential generated by the (1, −2) tidal mode. The most complicated solution of (1, 2) has been derived numerically by Matuura (1974) for a thermospheric wind system depending on activity indices (K_p, $F_{10,7}$) and using a realistic model for the electro-conductivities. The basic potential equation was $\operatorname{div}_H \mathbf{J}_H = 0$. The same equation has been used by Schieldge *et al.* (1973). They used a composition of (1, −2), (2, 2), (2, 3), and (2, 4) tidal modes and a realistic model for the electro-conductivities. A more indirect method for the computation of the large-scale ionospheric electric field has been used first in the pioneering work by Maeda (1955) and Kato (1956) and later on by Tarpley (1970) and Matsushita

(1971). This indirect method starts from $\mathbf{E} = \boldsymbol{\sigma}^{-1}\mathbf{j} - \mathbf{v}_n \times \mathbf{B}_0$ leading to curl $\boldsymbol{\sigma}^{-1}\mathbf{j} =$ curl $\mathbf{v}_n \times \mathbf{B}_0$. Models for $\mathbf{v}_n$ give informations about $\boldsymbol{\sigma}^{-1} \cdot \mathbf{j}$ and $\mathbf{j}$, while information about $\mathbf{j}$ can be used to determine $\mathbf{v}_n$. In both cases, $\mathbf{E}$ can be determined from the known fields $\boldsymbol{\sigma}^{-1} \cdot \mathbf{j}$ and $\mathbf{v}_n \times \mathbf{B}_0$.

In principle, also the method of 'equivalent circuits' developed by Stening (1968, 1973, 1977) and Kirchhoff (1975) can be used for the two-dimensional calculation of the symmetric dynamo-electric field.

3.1.4. *Results of the Two-Dimensional Symmetric Dynamo Models*

Two-dimensional dynamo models seem to be especially useful for the calculation of electrostatic ionospheric fields. The actual problem in the dynamo theory of ionospheric electric fields today is to determine which velocity fields are effective in dynamo actions. The symmetric theory gives the possibility to calculate the electrostatic potential for any given wind field. By comparison with the global distribution of measured electric fields (see Figure 4) or the daily variation of these fields for one station (see Figure 5), it is possible to estimate the contributions from different wind components.

Möhlmann tried with good success to reproduce the Richmond's map of the ionospheric electrostatic potential (compare the right-hand and left-hand side of Figure 4). He found that the (1, −2) and the (1, 1) tidal wind mode are effective in generating the large-scale ionospheric electrostatic field. It is interesting to note that a zonal part appears in Richmond's results. This is a new and unexpected result. The physical origin of this zonal part is unknown at present. A connection with zonal unipolar precipitation seems to be possible. For the global approximation of Richmonds map Möhlmann found

$$S = 3.77 \times 10^3 \sin\vartheta \cos^2\vartheta - 800 + 4S_{(1,-2)}(\vartheta, \varphi + 20°) + \\ + 24S_{(1,1)}(\vartheta, \varphi + 200°)$$

$S_{(1,-2)}$, $S_{(1,1)}$ electrostatic potential for the (1, −2), (1, 1) wind modes.

Concerning the dynamo effective winds the results of the computations of all authors agree in the following points:

– wind fields, equal or similar to the (1, −2) tidal mode seem to give an essential contribution to the dynamo-electric fields (Stening, 1973; Tarpley, 1970; Möhlmann, 1974, Schieldge *et al.*, 1973; Kirchhoff, 1975; Matuura, 1974; Dvinskikh, 1974),

– semi-diurnal tidal modes seem to play an essential role, too (Schieldge *et al.*, 1973; Kirchhoff, 1975),

– the thermospheric wind systems are effective, too, in dynamo-action (Matuura, 1974; Möhlmann, 1974; Kirchhoff, 1975).

But there is no reason to overestimate the degree of our knowledge: So far (to our knowledge) only Möhlmann has compared his results with Richmond's map. For other wind fields and the resulting electrostatic potentials equivalent current systems

have been used to check the accuracy. But this method is too insensitive (see below). If one compares the calculated daily variation of the ion drift velocity components produced by the electrostatic field with the observed values (see Figure 5) one can see that wind fields giving a good agreement between calculated and median regular equivalent *Sq* current systems do not show a good agreement with the electric field measurements. Very often one even sees contradictions. This situation has also been recognized by Richmond *et al.* (1976), who tried to improve this situation, but without any convincing success.

In spite of the limitations (see above) two-dimensional dynamo models very often have been used to calculate the horizontal current systems in the ionosphere. Generally, the quality of the calculations has been testified by comparison with equivalent current systems deduced from global measurements. Many authors have shown that two-dimensional models give a good agreement for median equivalent current systems. But a comparison of different calculations of this kind shows that this agreement does not depend very much on the composition of the tidal wind modes used by different authors, showing that the equivalent current systems are not sensitive enough to decide between different combinations of wind fields. One detail, visible in median regular equivalent current systems so far has not been explained by two-dimensional models and this is the shift of the foci on both hemispheres.

It has also been tried to use the two-dimensional dynamo model for the explanation of the seasonal and the UT-variations of the *Sq*-field (for an intensive discussion of these calculations see Mishin, 1976). For the seasonal variations, e.g., this kind of calculations leads to a very strong asymmetry between both hemispheres, which is in strong contrast to the observations, and shows the necessity to include coupling processes between both hemispheres in order to decrease the asymmetry (see Section 2.2.5).

3.2. Three-dimensional plasmaspheric current systems

3.2.1. *Basic Equations*

To simplify the calculations in the two-dimensional dynamo theory it has been assumed that $j_r = 0$ i.e. field-aligned electric currents $j_\parallel$ are not important. This condition is equivalent to the assumption that the velocity field, the magnetic field and the electric conductivity are symmetric for every pair of conjugated points; this is characteristical for symmetrical conditions.

In reality, however, all these parameters and also the electrostatic potential differ at geomagnetic conjugated points. Therefore is in principal $E_\parallel \neq 0$. Together with the fact $\sigma_\parallel \gg \sigma_\perp$ this leads to field-aligned currents and a current system, which is generally three-dimensional. The corresponding theory is the three-dimensional asymmetrical dynamo theory. The high electric field-aligned conductivity leads for conjugated points to a 'quasi-short-circuit' between both hemispheres and therefore to a weakening of the original potential differences. In this sense the field-aligned currents are quasi-short-circuit-currents. The intensity of these currents depends on

the degree of asymmetry. A contribution to the asymmetry of the electric field and the currents comes as well from the main geomagnetic field as from the electric conductivity and the neutral winds. The geomagnetic main field and the electric conductivity are rather well-known. On the other hand, the informations about the neutral wind are rather sparse. In order to understand the observations described in section 2 it would be interesting to know how great the contributions to the asymmetry are from the different sources. For this purpose every quantity has been divided into a symmetrical and into an antisymmetrical part relative to the geomagnetic equator. In this case one finds from Ohm's law

$$\mathbf{j} = (\boldsymbol{\sigma}^s + \boldsymbol{\sigma}^a)[\mathbf{E}^s + \mathbf{E}^a + (\mathbf{v}^s + \mathbf{v}^a) \times (\mathbf{B}^s + \mathbf{B}^a)] . \tag{3.13}$$

Here the indices at the top indicate the symmetrical (s) and the antisymmetrical (a) part relative to the equator. The symmetrical and antisymmetrical part of a scalar function (e.g. K) or a vector (e.g. $\mathbf{j}$) may be described by the values of these quantities at magnetic conjugated points in the northern and southern hemisphere (see De Witt, 1965; Maeda, 1974; Matveev, 1976a; Schäfer, 1978):

$$K_N = K^s + K^a, \qquad K_S = K^s - K^a,$$

$$j_x^s = \tfrac{1}{2}[j_x(\vartheta) - j_x(\pi - \vartheta)],$$

$$j_y^s = \tfrac{1}{2}[j_y(\vartheta) + j_y(\pi - \vartheta)],$$

$$j_x^a = \tfrac{1}{2}[j_x(\vartheta) + j_x(\pi - \vartheta)],$$

$$j_y^a = \tfrac{1}{2}[j_y(\vartheta) - j_y(\pi - \vartheta)].$$

By height-integration of the basic relation that the current system must be divergenceless (div $\mathbf{j} = 0$) one finds

$$j_r = \sin I \, j_\parallel = -\operatorname{div}_H \mathbf{J}_H^a \tag{3.14}$$

(I is the inclination) for the radial current density at the upper edge of the current carrying layer, if one assumes that no radial currents are flowing at the lower edge of the current layer. The horizontal height-integrated symmetrical current system $\mathbf{J}_H^s$ leads to $\operatorname{div}_H \mathbf{j}_H^s = 0$.

The quasi-short-circuit ($\sigma_\parallel / \sigma_\perp > 10^4$) leads to an averaging out of the antisymmetrical part of the polarization field ($E_p^s / E_p^A < 10^4$), that means that the antisymmetrical part of the electrostatic field may be neglected. Even in the three-dimensional dynamo theory the electrostatic field may be calculated from the two-dimensional potential equation resulting from the condition $\operatorname{div}_H \mathbf{J}_H^S = 0$ (see Matveev, 1971; Schieldge *et al.*, 1973; Matuura, 1974; Möhlmann, 1974). The three-dimensional current system may then be calculated from (3.14). Equation (3.14) may be rewritten in the form

$$\begin{aligned} j_r = -\operatorname{div}_H \{ & \boldsymbol{\Sigma}^a \mathbf{E}^s|_H + \boldsymbol{\Sigma}^a \mathbf{v}^s \times \mathbf{B}^a|_H + \boldsymbol{\Sigma}^s \mathbf{v}^a \times \mathbf{B}^a|_H + \\ & + \boldsymbol{\Sigma}^a \mathbf{v}^a \times \mathbf{B}^s|_H + \boldsymbol{\Sigma}^s \mathbf{v}^s \times \mathbf{B}^s|_H \} \end{aligned} \tag{3.15}$$

when $\boldsymbol{\Sigma}$ represents the height-integrated conductivity tensor. From this equation the different sources for field-aligned currents are obvious: the north-south asymmetry of the geomagnetic field and of the electric conductivity results in field-aligned currents changing with universal time. Furthermore, the seasonal asymmetries of the winds as well as of the electric conductivity produce a seasonal variation of the field-aligned currents.

Since the antisymmetrical part of the electric field may be neglected, this field cannot drive horizontal currents, which close the antisymmetrical current system $(\boldsymbol{\Sigma}\mathbf{v}\times\mathbf{B})^a$. As a result of the quasi-short-circuit the antisymmetric currents crossing the equator in the ionospheric current layer can be neglected, too. Consequently antisymmetric horizontal currents can be closed only along the geomagnetic field lines through the plasmasphere.

The methods to treat the three-dimensional problem have been developed, first of all in the papers of De Witt (1965), Cocks and Price (1969), Van Sabben (1966, 1969, 1970), Matveev (1971). On the other hand, Stening (1968) has developed quite another method to calculate the three-dimensional currents and the electric fields which is based on ideas developed in the electro-techniques, the equivalent circuit method. In his hierarchy of equations (see Section 3.1.) Möhlmann (1977) formulated a first-order-equation for the calculation of the geomagnetic field-aligned part of the electrostatic field.

Contributions to the three-dimensional dynamo-theory came from many additional authors: Nishida and Fukushima (1959), Dougherty (1963), K. Maeda and Murata (1965), Price (1968), Stening (1968, 1971, 1977), Mishin *et al.* (1968, 1970, 1971, 1976), Matveev (1970a, b 1976a, b), H. Maeda (1966, 1974), Schieldge *et al.* (1973), Schäfer (1978). In the following we intend to summarise the main results.

3.2.2. *Results*

Field-aligned currents which are produced due to the seasonal asymmetry of the electric conductivity have been estimated by Van Sabben (1970) and more in detail by Maeda (1974). This contribution may be calculated taking into consideration the first three terms on the right-hand side of (3.15). Maeda (1974) in his calculations used that wind model he found earlier (Maeda, 1966) from a solution of the indirect task of the dynamo theory, the conductivity was computed from CIRA-1965 and electron density measurements. The electric potential has been calculated using the equation $\mathrm{div}_H\, \mathbf{J}_H^S = 0$. The assumption of vertical geomagnetic field lines limits the results of Maeda to higher and median latitudes. Another limitation of his calculations results from the fact that he considered only UT-averaged current systems in dependence on season, i.e. the effect of the symmetric part of the **B**-field is averaged out.

Nevertheless the results of Maeda are fundamental and give a good possibility to estimate the contributions from the different terms in Equation (3.15). Figure 17 shows the resulting field-aligned current system. In Figure 17a the field-aligned currents resulting from the seasonal asymmetry of the electro-conductivity are

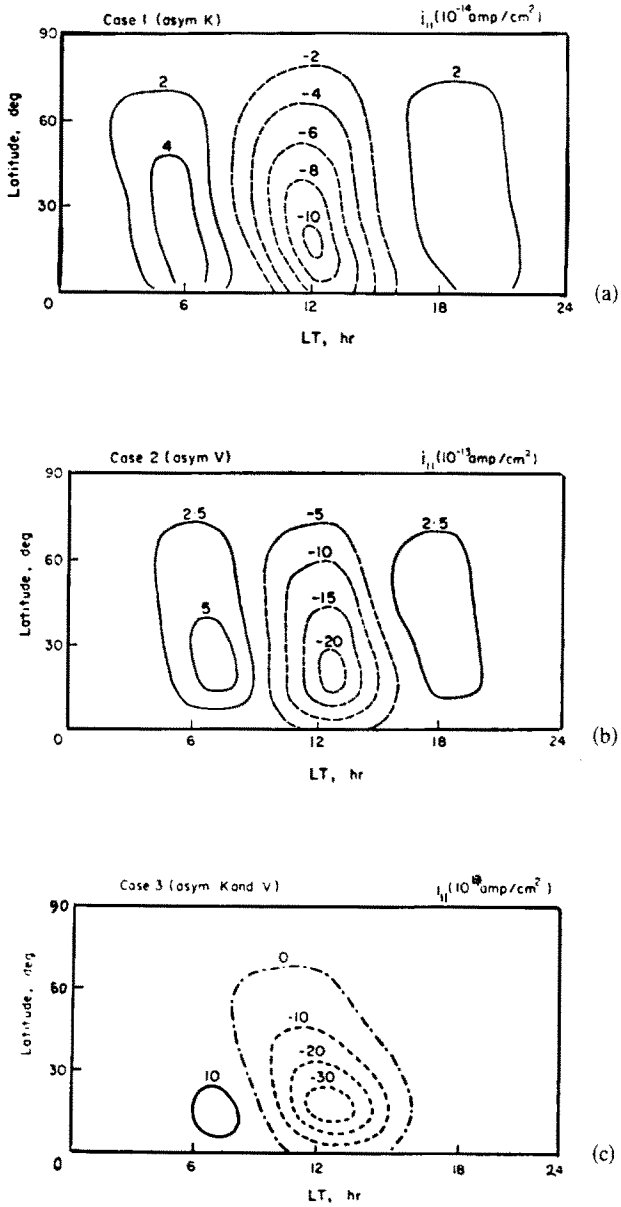

Fig. 17. Field-aligned current system after Maeda (1974) resulting from the seasonal asymmetry of the electric conductivity (case 1), of the winds (case 2), and both electric conductivity and winds (case 3).

shown and in Figure 17b those from the asymmetry of the winds (related to the second and third term on the right-hand side of (3.15)). In Figure 17c the field-aligned current system for the total (superposed) seasonal variation has been drawn. In the central part of the system the currents are flowing into the summer hemisphere, the centre of the current inflow is close to the focus of the equivalent *Sq*-currents and the current density is about 10^{-12} A cm^{-2}. Comparison of Figure

17a and Figure 17b shows that the asymmetry of the winds creates much more intense field-aligned currents than the asymmetry of the electric conductivity. All these features agree quite well with the facts known from observations (compare Section 2.2.5). On the other hand Maeda (1974) (see Figure 17) did not find intense field-aligned currents in the near equatorial region. In his picture currents showing a direction opposite to that of the central part only occur in medium latitudes on the morning and on the evening side. Furthermore, the centre of the currents in Figure 17 is situated at much lower latitudes than has to be expected from the observations. Maeda (1974) concluded that the night time part of the field-aligned current systems will become considerably less intensive if the daily variation of the conductivity is taken into consideration.

Recently, Schäfer (1978) also investigated the seasonal component of the field-aligned currents. In his model he used height-integrated conductivities in dependence on solar zenith angle given by Maeda and Murata (1968) and the tidal wind modes (1, 1), (1, −2), (2, 2) in a representation developed by Möhlmann (1975). To determine amplitude, phase and the relative contributions of these tidal modes, the magnetic field connected with $\mathbf{J}_H^a$ has been computed and compared with the antisymmetric part of the geomagnetic *Sq*-variation of several stations. The symmetric electrostatic field $\mathbf{E}^s$ has been computed using Möhlmann's method (1974, 1977) i.e. excluding the equatorial region. The geomagnetic field has been approximated by a centered dipole. That means that Schäfer (1978) took into account the first three terms on the right-hand side of (3.15). The results of the analytic computations (see Figure 18) again show field-aligned currents on the dayside, flowing into the summer hemisphere, with clear maxima around noon. The centre of the inflow lies near 30° latitude. The amplitude of the field-aligned current density is

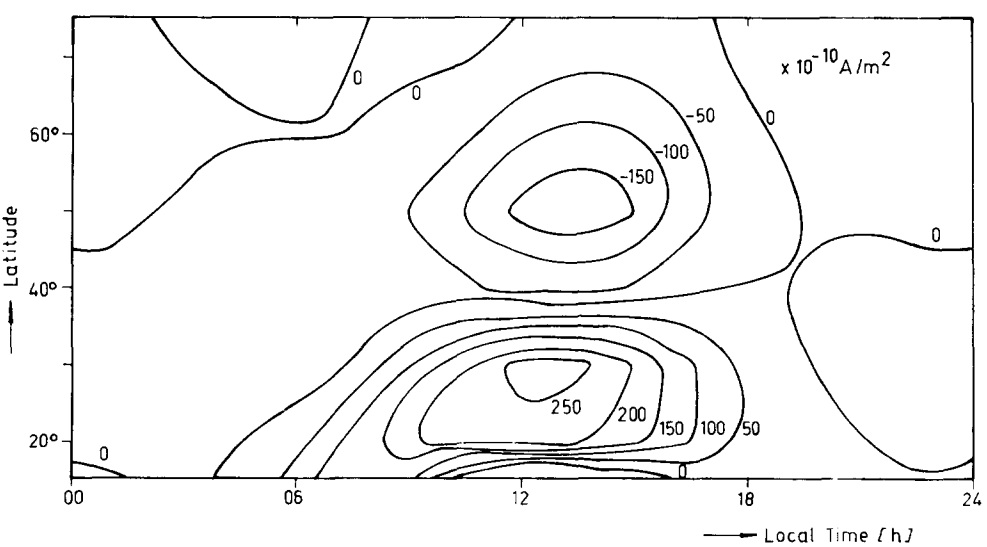

Fig. 18. Current density distribution of the threedimensional model for northern summer after Schäfer (1978).

of the order of 3×10^{-12} A cm^{-2}. In addition to the central part he found a centre of outflowing currents in higher latitudes near 50° latitude.

Another investigation taking into consideration seasonal as well as UT-variations has performed by Matveev (1976b). He built up a model considering only antisymmetrical winds i.e. considering the third and fourth term in Equation (3.15). The asymmetrical wind system changing with UT is calculated from a potential ψ with $\mathbf{v} = \text{grad } \psi$, tidal winds are not included. This potential ψ was estimated by solving the indirect task of the dynamo theory (calculating winds from geomagnetic equivalent currents) with the method of Maeda (1966). The geomagnetic main field has been approximated by a tilted dipole. The electric conductivity has been computed from electron density data in dependence on the zenith angle of the Sun. In this model the asymmetry of ionospheric winds is the dominating source for the field-aligned currents. For the structure of the field-aligned current, Matveev found a similar picture as given in Figure 17, but in addition a more equatorial region of currents with directions opposite to those of the currents in the centre. He also found strong dependencies on UT.

Another very interesting investigation about the seasonal and the UT-components of the field-aligned current system has been performed by Schieldge *et al.* (1973). These authors using data from a world-wide network of magnetic stations constructed maps of equivalent currents for four moments of universal time for August 5, 1958. The aim was to calculate that three-dimensional current system which gives for the horizontal calculated dynamo currents the best agreement with the equivalent current systems. For their global dynamo model they used a tilted dipole field, realistic conductivity distributions and height-dependent tidal winds. So, they took into account all terms in (3.15). The solution of the equation for the electrostatic potential is given in form of canonical series of harmonics S_n^m (cos θ) with n, m up to 8. For this task the authors practically had to solve an 'incorrect given task', which must be solved in principle using regularization methods. The authors solved this problem empirically and determined 8 parameters, which, in principle, give the amplitudes and phases of the wind system represented by them in form of four modes (1, −2), (2, 2), (2, 3), and (2, 4). This determination has been performed for any moment UT. Using this method the authors were not only able to calculate a system of horizontal dynamo currents, which is qualitatively close to the observations but also maps of the electrostatic fields associated with these computed currents. Unfortunately, the data for field-aligned currents and the polarization field have been published only for 03 : 30 UT. For this special moment the calculated map for the electrostatic potential considerably differs from the map presented in the Figure 4, which describes observed data (however averaged over UT). On the other hand, the gross-features of the calculated field-aligned currents seem to coincide quite well with those presented in Figure 17c. In this connection, it is interesting to mention that due to the authors the generation of the field-aligned currents is mainly due to the action of the neutral winds with mode (2, 3) and does not mainly come from the mode (1, −2) as Maeda (1974), Matveev (1976b), and Stening (1977) stated. According to

Schieldge *et al.* (1973) currents of the type presented in the Figure 17c in the near equatorial region will result in a daily variation of the Y-component of the ground-based magnetic field with an amplitude up to 20 nT in good correspondence with observations. These kinds of Y-variations in the near equatorial region due to field-aligned currents have also been investigated by Schäfer (1978) and Stening (1977).

Of course, it is of special interest to compare these results with those received by Stening (1968, 1971, 1977) using quite another method for the calculations. Stening investigated the UT-component as well in the horizontal as in the field-aligned currents. As velocity field he used the (1, −2) mode, the magnetic field is given by the IGRF-1965 and his conductivity calculations included dependencies on the magnetic field as well as on solar zenith angle. He calculated field-aligned current systems for three different seasons (summer, winter, equinox) and for three moments of UT corresponding to local noon for the Asian/Australian, European/African, and American longitudinal sectors (02:00; 10:00; 18:00 UT). The results of Stening's calculation are presented in Figure 19. About the degree of similarity or disagreement with Figure 17b or 18 the reader should develop its own opinion. In order to understand the cause for the differences it is necessary to consider the approximations for the calculations and in the model: the winds are tidal winds of (1, −2)-mode and do not change with season; the dynamo-emf. in both hemispheres are identical and have been determined from the equation $e = (e_N \cdot G_N + e_S \cdot G_S)/(G_N + G_S)$ where e_N, e_S are the emf in the northern and southern hemispheres and G_N, G_S are electric conductivities averaged along the line of force.

These results clearly demonstrate the strong dependence of field-aligned currents on universal time and also the strong dependence on the wind (see Figure 19 first and last picture). Furthermore, Stening found strong field-aligned currents close to the equator with opposite direction to those in medium latitudes. As Stening (1977) has shown these field-aligned near-equatorial currents create variations in the ground-based Y-component in that way as they have been observed in the American and European/African zone. This finding is not unexpected since also Schieldge *et al.* (1973) were able to explain these Y-variations with a field-aligned current system similar to that given in Figure 17c. In spite of some shortcomings and disadvantages the results of Stening give an interesting contribution to the whole picture.

In conclusion one has to state that all these calculations are only first steps, and this development is quite at the beginning. Nevertheless, the results of Maeda (1974), Matveev (1976), Schieldge *et al.* (1973), Stening (1977), and Schäfer (1978) give already informations about the seasonal component of the field-aligned currents. It also should be mentioned that these results are not too far from the empirical model described in Section 2.2.5. Figure 20 tries to summarize these results schematically for northern summer. Inside the plasmasphere ($L \approx 1.5$) on the dayside we have field-aligned currents near local noon flowing steadily into the summer hemisphere. Outside of this central part towards morning and evening and towards other latitudes, we have more diffuse field-aligned current regions where the currents flow

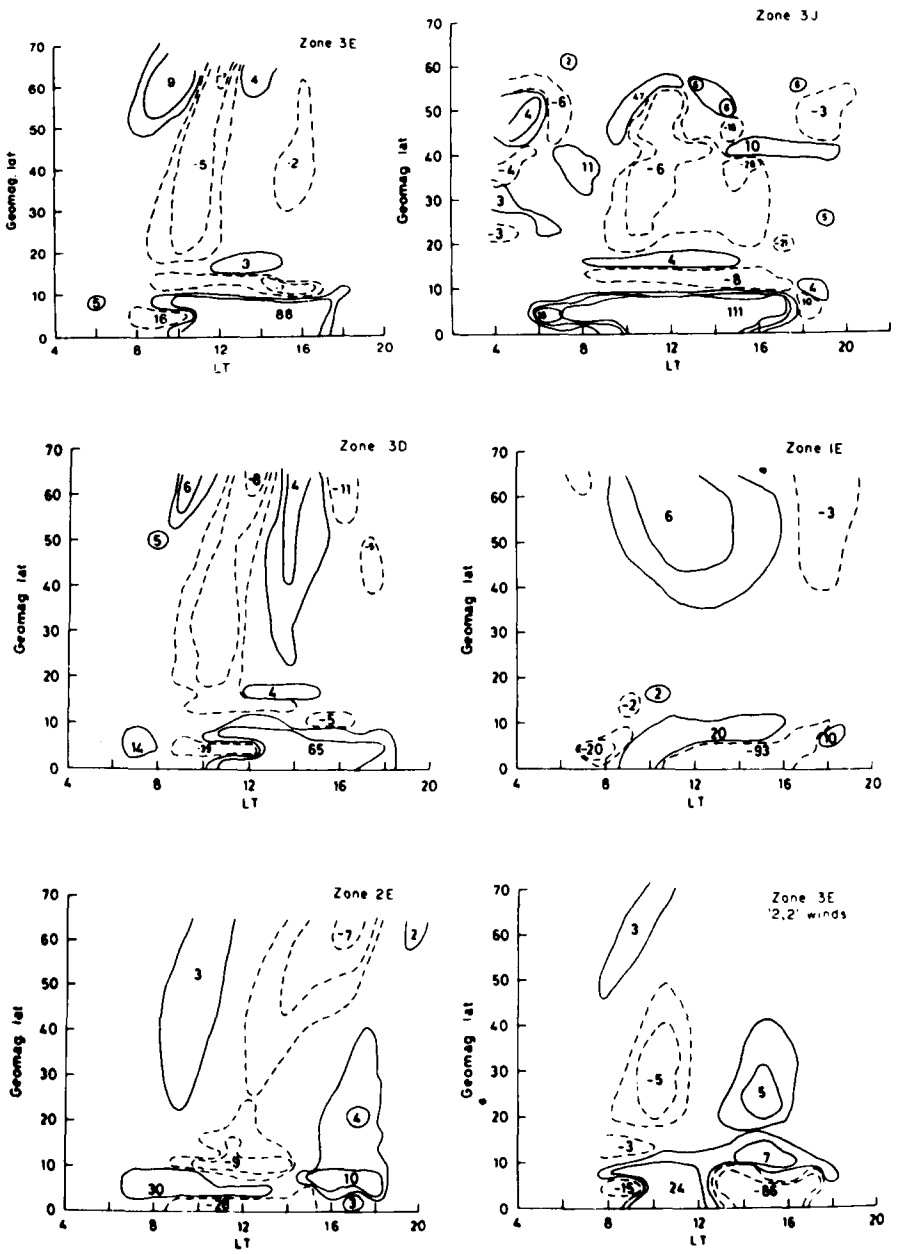

Fig. 19. Field-aligned current systems (10^{-12} A/cm^{-2}) after Stening (1977) for different seasons (*E*, *J*, *D*), geomagnetic longitudinal sectors (zone 1–3), and winds.

in the opposite direction. These field-aligned currents are closed by ionospheric currents mainly in the *E*-layer. This three-dimensional current system is totally embedded into the plasmasphere.

The field-aligned currents combined with the UT-variations need further investigations but, in principle, seem to be explainable by the three-dimensional dynamo

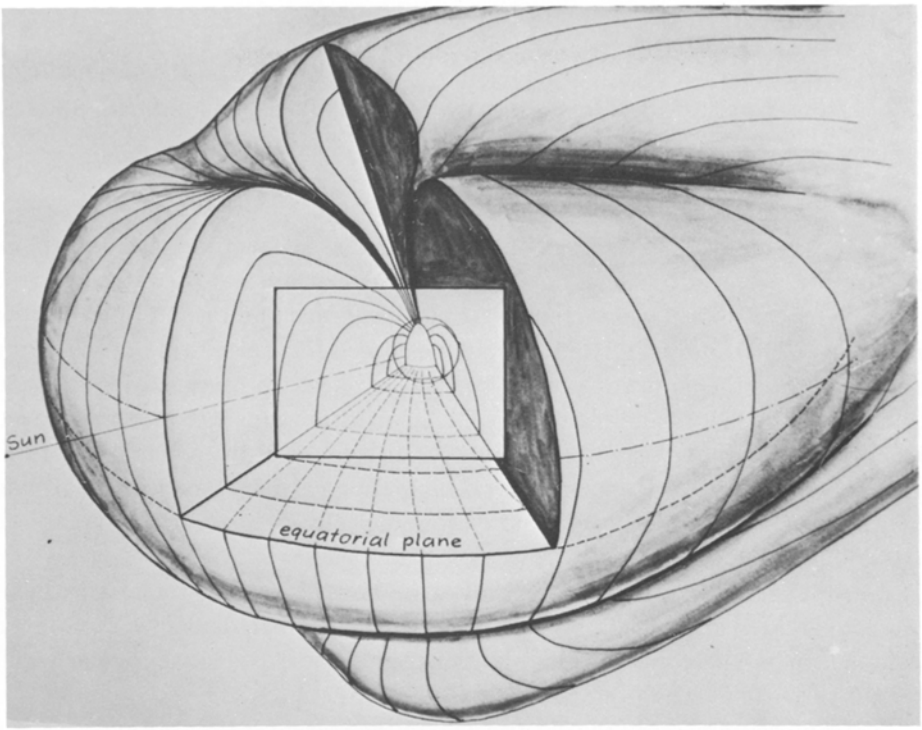

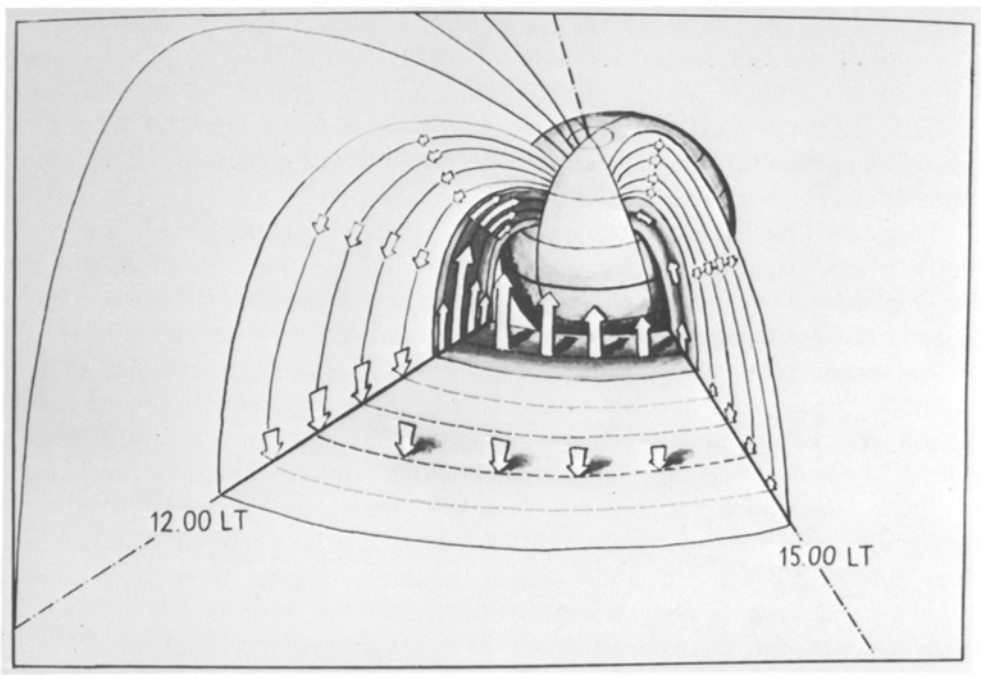

Fig. 20. Scheme of the threedimensional system for northern summer deduced from all informations available. (a) Showing the position within the magnetosphere. (b) Showing more details. In (b) only those field lines, carrying field-aligned currents have been drawn. The arrows indicate the direction and strength of the field-aligned currents in the equatorial plane.

theory. On the other hand, the constant part of field-aligned currents which has been deduced from experiments seems to be only explainable using additional physical processes.

4. Summary

The study of large-scale fields in medium latitudes has a rather long history. In the earliest epoch averaged *Sq*-fields have been investigated and interpreted on the base of a two-dimensional dynamo model using linear assumptions for the electric conductivity of the ionosphere and very simple models for the neutral winds. During the second epoch the anisotropy of the ionospheric electrical conductivity has been included into the theory and the models for the neutral winds have been improved using as well tidal theory as solutions of the indirect task of the dynamo theory. It became obvious during this epoch that two-dimensional dynamo models can explain nearly all facts, which have been found morphologically for averaged *Sq*-fields (see Section 2.2.5(I)).

During the recent decade new or improved methods to measure e.g. electric fields (e.g. incoherent scatter facilities) and to investigate great data files have been developed. Using these methods informations about the existence of regular variations of the *Sq*-field and the electric field have been found:

- Direct measurements of the electric field by incoherent scatter stations gave the possibility to construct a first global map of the distribution of the (averaged) electric field in the quiet plasmasphere (see Figure 4).
- Annual and semi-annual variations of the *Sq*-field characteristics have been determined (variations of the total currents and the position of the vortices, variations in the time differences between both foci etc. (see Section 2.2.5)).
- UT-variations of the *Sq*-field have been identified (modulation of the total currents and the position of the vortices etc. (see Section 2.2.5)).

The seasonal and UT-variations are due to asymmetric conditions on the northern and southern hemisphere. All attempts to describe also these variations with a two-dimensional dynamo model did not lead to any success, but showed a strong theoretical overestimation of the asymmetries in comparison with the measurements of the *Sq*-field. The only possible conclusion was to assume the existence of an additional process, which leads to a decrease of the asymmetry between both hemispheres. Such a process is given by the coupling between both hemispheres through the high-conducting magnetic field lines. Therefore, it must be concluded that three-dimensional plasmaspheric current systems are needed in order to explain the regular variations of the *Sq*-field. Rough estimations showed that such a three-dimensional dynamo model should be able to explain most of the new morphological findings about regular variations of the *Sq*-field. So far, quantitatively, only some first approximations of such a three-dimensional model have been computed (see Section 3.2).

Concerning the electric fields the coupling between both hemispheres leads to a quasi-short-circuit. Therefore, the anti-symmetric components of the electric fields

must be rather small and the symmetric components calculated with a two-dimensional dynamo model can be aspected to be good approximations. A combination of dynamo-effective wind modes giving a good approximation of the global **E**-field has been found (see Figure 4), but, on the other hand, the agreement with measurements at single stations is not at all satisfactory.

The morphological results described in Section 2 and the theoretical calculations compiled in Section 3 give the possibility to construct a three-dimensional current system (see Figure 20): Inside the plasmasphere ($L \approx 1.5$) on the dayside there exists a concentrated region of field-aligned currents near local noon flowing steadily into the summer hemisphere. Outside of this central part towards morning and evening and towards other latitudes we have a more diffuse field-aligned current region, where the currents flow in opposite direction. The characteristic amplitude of the current density of these field-aligned currents is about 10^{-12} A cm^{-2}, depending on universal time and season. To understand the regular variations of the Sq-field one has to assume a seasonal component of the field-aligned current flowing into the summer hemisphere and being concentrated close to the foci of the Sq-vortices. In their central part the UT-dependent field-aligned currents flow into the northern hemisphere for the period 05 : 00–19 : 00 UT. For the period 19 : 00–05 : 00 UT these currents decrease and change their sign. There are some indications for the existence of a time- and season-independent component of the field-aligned currents flowing always into the northern hemisphere.

The tasks to be solved in near future are:

– To improve our knowledge about the electric field and its variations by performing simultaneous, coordinated measurements; to prove the existence of field-aligned currents inside the dayside plasmasphere;

– to identify and separate non-plasmaspheric contributions from the Sq-variations during daytime;

– to improve the methods needed to solve the three-dimensional dynamo equations and especially to improve the models for ionospheric winds, electric conductivity and for the main geomagnetic field; to introduce more realistic boundary conditions for high and low latitudes.

In conclusion, one can state that during the recent decade there has been a very interesting development of the old problem of the Sq-system giving a good fundament to treat interesting magnetospheric problems in near future.

References

Adam, N. V., Benkova, N. P., and Orlov, V. P. *et al.*: 1964, 'Geomagnetic Field in Altitudes from 0 to 15 000 km for the Epoch 1955', Preprint Izmiran, pp. 35–64 (in Russian).

Afraimovitch, E. B., Bazarzhapov, A. D., Mishin, V. M., Nemtsova, E. I., Osipov, N. K., Platanov, M. L., Urbanovitch, V. D.: 1966, *Geomagnitnije Issledovanija* **8**, 31 (in Russian).

Akasofu, S.-I.: 1977, *The Physics of Magnetospheric Substorms*, D. Reidel Publ. Co., Dordrecht, Holland.

Akasofu, S.-I. and Chapman, S.: 1972, *Solar Terrestrial Physics*, Oxford Univ. Press, Clarendon, London, New York.

Akopjan, A. V.: 1966, 'Role of the Daily Precession of the Geomagnetic Dipole for the Generation of *Sq*-Variation', in *Zemnoj Magnetism, Polarnije Sijanija i UNTch*, Irkutsk SibIzmir, pp. 84–89 (in Russian).
Baker, W. G. and Martyn, D. F.: 1953, *Phil. Trans Roy. Soc. London* **A246**, 281.
Bazarzhapov, A. D., Levadnij, V. T., and Mishin, V. M.: 1969, Mean *Sq*-field during solstice of the IGY, *Issled. Geomagn. Aeron. Fizike Solntsa, Irkutsk* **5**, 28 (in Russian).
Bazarzhapov, A. D., Matveev, M. I., and Mishin, V. M.: 1979, *Geomagnetic Variations and Storms*, Nauka, Novosibirsk (in Russian).
Benkova, N. P.: 1941, *Quiet Solar-Daily Geomagnetic Variations*, Gidrometeoisdat, Leningrad (in Russian).
Bhargava, B. N. and Jacob, A.: 1971, *J. Geomagn. Geoelectr.* **23**, 249.
Blanc, M. and Amayenc, P.: 1976, in J. J. Burger, A. Pedersen, and B. Battrick (eds.), *Atmospheric Physics from Spacelab*, D. Reidel Publ. Co., Dordrecht, Holland, p. 61.
Blum, P. W. and Harris, I.: 1972, 'The Global Wind System in the Thermosphere', *Space Res.* **XIII**, and NASA Doc. X-621-73-25.
Blum, P. W. and Harris, I.: 1975a, *J. Atmospheric Terrest. Phys.* **37**, 193.
Blum, P. W. and Harris, I.: 1975b, *J. Atmospheric Terrest. Phys.* **37**, 213.
Carpenter, D. L.: 1978, *J. Geophys. Res.* **83**, 1558.
Carpenter, L. A. and Kirchhoff, V. W. J. H.: 1975, *J. Geophys. Res.* **80**, 1810.
Chapman, S. and Bartels, J.: 1940, *Geomagnetism*, Part 1, 2, Oxford Univ. Press, Clarendon, London, New York.
Chapman, S. and Lindzen, R. S.: 1970, *Atmospheric Tides*, D. Reidel Publ. Co., Dordrecht, Holland.
Cocks, A. C. and Price, A. T.: 1969, *Planetary Space Sci.* **17**, 471.
Cole, K. D. and Thomas, J. A.: 1968, *Planetary Space Sci.* **16**, 1357.
De Witt, R. N.: 1965, 'Dynamo Action in Ionosphere and Motions of the Magnetospheric Plasma', Scientif. Rep. NSF GP 2721, Geophys. Inst. Univ. of Alaska.
Dougherty, J. P.: 1963, *J. Geophys. Res.* **68**, 2383.
Dvinskich, R. C.: 1974, *Issled. Geomagn. Aeron. Fizike Solntsa, Irkutsk* **34**, 58 (in Russian).
Fukushima, N. and Kamide, Y.: 1973, *Radio Sci.* **8**, 1013.
Geisler, J. E.: 1966, *J. Atmospheric Terrest. Phys.* **28**, 703.
Geisler, J. E.: 1967, *J. Atmospheric Terrest. Phys.* **29**, 1469.
Glushakov, M. L. and Samochin, M. V.: 1974, *Geomagn. Aeron.* **14**, 584 (in Russian).
Gringauz, K. I. and Besrukich, V. V.: 1977, *Geomagn. Aeron.* **5**, 784 (in Russian).
Gurnett, D. A.: 1972, 'Electric Field and Plasma Observations in the Magnetosphere', Preprint Univ. of Iowa, No. 72–14..
Hasegawa, M.: 1936, *Proc. Imp. Acad. Tokyo* **12**, 88–90, 185–188, 221–224, 225–228, 277–280.
Hasegawa, M.: 1937, *Proc. Imp. Acad. Tokyo* **13**, 65–68, 69–73, 311–315.
Hasegawa, M.: 1938, *Proc. Imp. Acad. Tokyo* **14**, 4–8.
Hasegawa, M.: 1965, *J. Geophys. Res.* **65**, 1437.
Hasegawa, M. and Ota, M.: 1950, *LATME Bull.* **13**, 426.
Heelis, R. A. *et al.*: 1973, *Planetary Space Sci.* **22**, 743.
Heppner, J. P.: 1972, *J. Geophys. Res.* **77**, 4877.
Heppner, J. P.: 1977, *J. Geophys. Res.* **82**, 7, 1115.
Hines, C. D.: 1965, *J. Geophys. Res.* **70**, 177.
Iijima, T. and Potemra, T. A.: 1976, *J. Geophys. Res.* **81**, 2165.
Izmiran, Mesjatchnij prognoz MPTch. M.: 1958, *Izmiran*, pp. 1–12 (in Russian).
Izmiran, Mesjatchnij prognoz MPTch. M.: 1963, *Izmiran*, p. 9 (in Russian).
Jacchia, L. G.: 1965, *Space Res.* **5**, 1152.
Kane, R. P.: 1971, *J. Atmospheric Terrest. Phys.* **33**, 319.
Kane, R. P.: 1976a, *Space Sci. Rev.* **18**, 413.
Kane, R. P.: 1976b, *Ind. J. Radio Space Phys.* **5**, 6.
Kato, S.: 1956, *J. Geomagn. Geoelectr.* **8**, 24.
Kirchhoff, V. W. J. H.: 1975, 'Electric Fields in the Ionosphere', PSU-IRL-SCI-438, The Pennsylvania State University.
Kohl, H. and King, J. W.: 1967, *J. Atmospheric Terrest. Phys.* **29**, 1045.

Lindzen, R. S.: 1967, *J. Geophys. Res.* **72**, 1591.
Lindzen, R. S.: 1971, *Geophys. Fluid Dyn.* **2**, 89.
Lyatskij, W. B. and Maltsev, J. P.: 1975, *Geomagn. Aeron.* **15**, 118 (in Russian).
Maeda, H.: 1955, *J. Geomagn. Geoelectr.* **7**, 121.
Maeda, H.: 1957, *J. Geomagn. Geoelectr.* **9**, 86.
Maeda, H.: 1966, *J. Atmospheric Sci.* **23**, 363.
Maeda, H.: 1974, *J. Atmospheric Terrest. Phys.* **36**, 1395.
Maeda, H. and Murata, H.: 1968, *J. Geophys. Res.* **73**, 1077.
Maeda, H. *et al.*: 1979, 'Electric Fields and Neutral Winds in the Ionospheric Dynamo Region', WDC-C2 Data Book No. 2.
Maeda, K. and Murata, H.: 1965, *Rept. Ionosph. Space Res. Japan* **19**, 272.
Matsushita, S.: 1969, *Radio Sci.* **4**, 771.
Matsushita, S.: 1971, *Radio Sci.* **6**, 279.
Matsushita, S.: 1975, *EOS Trans. AGU* **56**, 621.
Matsushita, S. and Balsley, B.: 1972, *Planetary Space Sci.* **20**, 1259.
Matsushita, S. and Maeda, H.: 1965, *J. Geophys. Res.* **70**, 2535.
Matsushita, S. and Tarpley, J. D.: 1970, *J. Geophys. Res.* **75**, 5433.
Matuura, N.: 1974, *J. Geophys. Res.* **79**, 4679.
Matveev, M. I.: 1970a, *Issled. Geomagn. Aeron. Fizike Solntsa, Irkutsk* **11**, 102 (in Russian).
Matveev, M. I.: 1970b, *Issled. Geomagn. Aeron. Fizike Solntsa, Irkutsk* **11**, 116 (in Russian).
Matveev, M. I.: 1971, *Gerlands Beitr. Geophys.* **80**, 155.
Matveev, M. I.: 1974, *Issled. Geomagn. Aeron. Fizike Solntsa, Irkutsk* **30**, 49 (in Russian).
Matveev, M. I.: 1976a, *Issled. Geomagn. Aeron. Fizike Solntsa, Irkutsk* **39**, 112 (in Russian).
Matveev, M. I.: 1976b, *Issled. Geomagn. Aeron. Fizike Solntsa, Irkutsk* **39**, 118 (in Russian).
Mishin, V. M.: 1968, *Geomagn. Aeron.* **8**, 134 (in Russian).
Mishin, V. M.: 1970, 'Dynamics of Global *Sq*-Fields and Field-Aligned Current in the Earth's Magnetosphere', IFZ, AN SSSR and Ph.D. Thesis, Irkutsk (in Russian).
Mishin, V. M.: 1976, *Quiet Geomagnetic Variations and Currents in the Magnetosphere*, Nauka, Sib. Otdel. Novosibirsk (in Russian).
Mishin, V. M., Bazarzhapov, A. D., Matveev, M. I., Popov, G. V., Tubalova, V. M., and Nemtsova, E. I.: 1971, *Gerl. Beitr. Geophys.* **80**, 171.
Mishin, V. M., Bazarzhapov, A. D., Nemtsova, E. J., and Anistratenko, A. A.: 1975, *Issled. Geomagn. Aeron. Fizike Solntsa, Irkutsk* **36**, 18 (in Russian).
Mishin, V. M., Bazarzhapov, A. D., Nemtsova, E. J., and Sholpo, M. E.: 1966, 'Mean Maps of *Sq*-Currents from Data During Solstice of the IGY', in *Zemnoj Magnetism, Polarnije Sijanija i UNTch* Irkutsk SibIzmir, pp. 49–61 (in Russian).
Mishin, V. M. and Erushenko, A. I.: 1966, 'Daily Variation of Electro-Conductivity in the *E*-Layer of the Ionosphere', in *Zemnoj Magnetism, Polarnije Sijanija i UNTch*, Irkutsk SibIzmir, pp. 78–83 (in Russian).
Mishin, V. M., Matveev, M. I., and Bazarzhapov, A. D.: 1970, *Issled. Geomagn. Aeron. Fizike Solntsa, Irkutsk* **11**, 80 (in Russian).
Mishin, V. M. and Nemtsova, E. J.: 1966, 'The UT-Component of the *Sq*-Variation with Data II of the IGY', in *Zemnoj Magnetism, Polarnije Sijanija i UNTch*, Irkutsk SibImir, pp. 62–77 (in Russian).
Mishin, V. M., Nemtsova, E. J., and Urbanovich, V. D.: 1966, 'Seasonal Variation of *Sq*-Currents with Data of the IGY', in *Zemnoj Magnetism, Polarnije Sijanija i UNTch*, Irkutsk SibIzmir, pp. 90–101 (in Russian).
Möhlmann, D.: 1971, 'About the Dynamo Theory of the Geomagnetic Sq-Variations', Dissertation, Karl-Marx-Univ. Leipzig (in German).
Möhlmann, D.: 1974, *Gerlands Beitr. Geophys.* **83**, 101.
Möhlmann, D.: 1976, *Gerlands Beitr. Geophys.* **85**, 249.
Möhlmann, D.: 1977, *J. Atmospheric Terrest. Phys.* **39**, 1325.
Möhlmann, D. and Wagner, C.-U.: 1970, *J. Atmospheric Terrest. Phys.* **32**, 445.
Mozer, F. S.: 1973, *Rev. Geophys. Space Phys.* **11**, 755.
Mozer, F. S. and Lucht, P.: 1974, *J. Geophys. Res.* **79**, 1001.
Nagata, T. and Sugiura, M.: 1948, *Geophys. Note Univ. Tokyo* **36**, 15.

Nemtsova, E. J.: 1966, *Geomagnitnije Issledovanija* **8**, 52 (in Russian).
Nemtsova, E. J. and Mishin, V. M.: 1970, *Issled. Geomagn. Aeron. Fizike Solntsa, Irkutsk* **11**, 221 (in Russian).
Nishida, A.: 1971, *Cosmic Electrodynamics* **2**, 350.
Nishida, A. and Fukushima, N.: 1959, *Rept. Ionosph. Space Res. Japan* **13**, 273.
Olson, W. P.: 1970, *Planetary Space Sci.* **18**, 1471.
Price, A. T.: 1968, *Geophys. J. Roy. Astron. Soc.* **15**, 93.
Price, A. T. and Wilkins, G. A.: 1963, *Phil. Trans. Roy. Soc.* **A256**, 31.
Richmond, A. D.: 1976, *J. Geophys. Res.* **81**, 1447.
Richmond, A. D., Matsushita, S., and Tarpley, J. D.: 1976, *J. Geophys. Res.* **81**, 547.
Rishbeth, H.: 1971, *Planetary Space Sci.* **19**, 263.
Sarabhai, V. and Nair, K. N.: 1969, *Nature* **223**, 603.
Schäfer, K.: 1978, *J. Atmospheric Terrest. Phys.* **40**, 755.
Schieldge, J. P., Venkateswaran, S. V., and Richmond, A. D.: 1973, *J. Atmospheric Terrest. Phys.* **35**, 1045.
Stening, R. J.: 1968, *Planetary Space Sci.* **16**, 717.
Stening, R. J.: 1969, *Planetary Space Sci.* **17**, 889.
Stening, R. J.: 1971, *Radio Sci.* **6**, 133.
Stening, R. J.: 1973, *Planetary Space Sci.* **21**, 1897.
Stening, R. J.: 1977, *J. Atmospheric Terrest. Phys.* **39**, 933.
Stern, D. P.: 1977, *Rev. Geophys. Space Phys.* **15**, 156.
Tarpley, J. D.: 1970, *Planetary Space Sci.* **18**, 1075.
Van Sabben, D.: 1966, *J. Atmospheric Terrest. Phys.* **28**, 965.
Van Sabben, D.: 1969, *J. Atmospheric Terrest. Phys.* **31**, 469.
Van Sabben, D.: 1970, *J. Atmospheric Terrest. Phys.* **32**, 1331.
Vertlib, A. B. and Wagner, C.-U.: 1970, *Geomagn. Aeron.* **10**, 649 (in Russian).
Vertlib, A. B. and Wagner, C.-U.: 1977, *Gerlands Beitr. Geophys.* **86**, 373.
Volland, H. and Mayr, H. G.: 1973, *Ann. Geophys.* **29**, 61.
Volland, H. and Mayr, H. G.: 1974, *Radio Sci.* **9**, 263.
Volland, H.: 1976a, *J. Atmospheric Terrest. Phys.* **38**, 869.
Volland, H.: 1976b, *J. Geophys. Res.* **81**, 1621.
Wagner, C.-U.: 1968, The Model of the Asymmetric Atmospheric Dynamo and Its Application to the Determination of the Conductivity of the Ionospheric Plasma from Geomagnetic *Sq*-Variations', Abh. Nr. 37, Geomagn. Inst. Potsdam, Doctor Thesis (in German).
Wagner, C.-U.: 1968, *J. Atmospheric Terrest. Phys.* **30**, 579.
Wagner, C.-U.: 1969, *Gerlands Beitr. Geophys.* **78**, 120.
Wagner, C. U.: 1971, *J. Atmospheric Terrest. Phys.* **33**, 751.
Wagner, C.-U.: 1977, *Phys. Solariterr. Potsdam* **5**, 3.
Wagner, C.-U.: 1978, 'Satellite Measurements Concerning Ionospheric-Magnetospheric Current Systems', HHI-STP-Report 11, Berlin.
Wagner, C.-U., Schäfer, K.: 1980, 'Measurements of Ionospheric and Plasmaspheric Electric Fields under Quiet Conditions', *Phys. Solariterr.* (in preparation).
Wiese, H.: 1951, *Z. Meteorologie* **5**, 373 (in German).
Yanagihara, K.: 1971, *Memo. Kakioka Magn. Obs.* **14**, 1.
Zaitzev, A. N.: 1968, *Geomagn. Aeron.* **6**, 117 (in Russian).